X-551-72-372

PREPRINT

NASA TM X- 66134

ONE WAY AND TWO WAY VHF RANGING SYSTEM PERFORMANCE FOR TRACKING AND DATA RELAY APPLICATION

JOHN W. BRYAN

CESAR A. FILIPPI

SEPTEMBER 1972

GSFC

GODDARD SPACE FLIGHT CENTER

GREENBELT, MARYLAND

X-551-72-372

ONE WAY AND TWO WAY VHF RANGING SYSTEM PERFORMANCE FOR TRACKING AND DATA RELAY APPLICATIONS

John W. Bryan
Flight Mission Analysis Branch
Goddard Space Flight Center

Cesar A. Filippi
Advanced Systems Analysis Office
The Magnavox Company

Goddard Space Flight Center
Greenbelt, Maryland

ONE WAY AND TWO WAY VHF RANGING SYSTEM PERFORMANCE FOR TRACKING AND DATA RELAY APPLICATIONS

John W. Bryan
Flight Mission Analysis Branch
Goddard Space Flight Center

Cesar A. Filippi
Advanced Systems Analysis Office
The Magnavox Company

ABSTRACT

The trajectory of an orbiting spacecraft is determined from an Orbit Determination Program (ODP). Two inputs to this program, among others, are the range and range rate relative to some known location. The uncertainties in the determination of the range and range rate reflects directly into the uncertainty in the orbit determination. This report presents an analysis of VHF ranging systems when applied to the Tracking and Data Relay Satellite System (TDRSS). The analysis is applied not only to the convention two way range and range rate system but also to one way range rate and a new data type range-difference.

The major contributor to the range rate error is the uncertainty in the speed of light. For high signal to noise ratios the measurement uncertainties due to the system oscillators predominate. Under the constraint of matched phase locked loop errors the 1 way range rate system is superior to the 2 way system. For low signal to noise ratios the thermal noise predominates and the 2-way GRARR and 1 way systems are compatible. However under these conditions the coherent user system is superior to either of these.

The range uncertainties are also predominated by our knowledge of the velocity of light. For high signal to noise ratios the uncertainty in the range measurement is governed by the time jitter and by thermal noise for low signal to noise ratios.

For the new data type (range difference) the error is predominated by thermal noise at low signal to noise ratios and by time jitter at high signal to noise ratios.

Prev. Page Blank

TABLE OF CONTENTS

TABLES

P. P. Blank

CONTENTS—(continued)

ILLUSTRATIONS

ONE WAY AND TWO WAY VHF RANGING PERFORMANCE FOR TRACKING AND DATA RELAY APPLICATIONS

1. INTRODUCTION

In the NASA ground-centralized tracking systems, the trajectory of an orbiting or maneuvering spacecraft is ascertained by measuring certain parameters that reflect the spacecraft orbital motion and using these measurements, with the possible inclusion of some data smoothing and editing operations as inputs to an orbit determination program. A conventional set of measured parameters is the slant range and range rate of the spacecraft relative to ground stations or some other reference point such as a stationary relay satellite. The tracking accuracy is governed by the arithmetic and measurement errors present in these measured parameters as well as by the location uncertainties of the ground stations or reference satellites.

The tracking accuracy performance has been recently studied by The Trajectory Analysis and Geodynamics Division at GSFC employing representative range and/or range rate data samples for both an all-ground and a ground/relay-satellite tracking network.[1, 2, 3] The study results revealed the feasibility of relay satellite tracking systems (TDRS), as well as high accuracy capabilities when employing even range rate only as the tracking data relayed by two simultaneous satellites. For example, tabulated below are some orbit determination program simulation results of the tracking accuracy performance study when using one or two synchronous satellites to track a 100 n.m. circular-orbit spacecraft. Summarized in Table 1 is the error performance in tracking the relay satellite by an all-ground tracking network, as a function of the ground station geometry and the tracking period. It should be mentioned that the station location uncertainties and tracking data errors assumed to derive the synchronous satellite errors are representative of existing NASA tracking station facilities and tracking system capabilities. We then summarized in Table 2 the error performance in tracking the 185 km spacecraft with the relay satellite network using either range and range rate or range rate only data, as a function of the relay satellite location uncertainty and the tracking period. Again, the satellite location uncertainties and the tracking errors assumed are representative of NASA tracking system capabilities.

The purpose of this report is to evaluate the error performance capabilities of 1-way vs 2-way ranging systems for TDRS applications, with particular attention to the extraction of range rate data pertinent to a USER spacecraft. The aforesaid study results motivate the interest in TDRS tracking systems based on

TABLE I

Error Performance (1σ Uncertainty) When Tracking A Synchronous Satellite by An All-Ground Tracking Network

(a) Two Simultaneous Ground Stations

	24-hr tracking	12-hr tracking	3-hr tracking
Best geometry	340 meters	350 meters	580 meters
Worst geometry	1200 meters	1300 meters	2600 meters

(b) Two Switching Ground Stations

	24-hr tracking	12-hr tracking	3-hr tracking
Best geometry	340 meters	390 meters	54200 meters
Worst geometry	900 meters	1780 meters	55700 meters

(c) One Ground Station

	24-hr tracking	12-hr tracking	3-hr tracking
Best geometry	11100 meters	14300 meters	55700 meters
Worst geometry	16800 meters	27500 meters	60000 meters

TABLE II

Error Performance (1σ Uncertainty) When Tracking A 185 km High Spacecraft (User) Via A Synchronous Satellite Tracking Network

Range and Range Rate Data

TDRS RMS Errors	User RMS Errors With One TDRS		User RMS Errors With Two TDRS	
	1-min	5-min	1-min	5-min
500 m	3.6 km	0.9 km	2.1 km	0.2 km
1000 m	3.6 km	0.9 km	2.9 km	0.3 km
2000 m	3.9 km	1.2 km	3.8 km	0.5 km
Range Rate Data Only				
500 m	6.0 km	4.9 km	4.1 km	0.2 km
1000 m	6.0 km	4.9 km	4.1 km	0.2 km
2000 m	6.9 km	4.9 km	4.3 km	0.2 km

range rate data only, and the choice between 1-way vs 2-way systems is the natural question that follows since both are capable of yielding such tracking data. The 2-way ranging systems can also provide range data, but a 1-way ranging system would simplify the ranging signal processing and system design while supplying a new data type (range-difference) when two TDRS are simultaneously available. A comparison of 2-way vs 1-way ranging performance is thus motivated. The first sections that follow will concentrate on the range rate extraction and error performance, while the last sections consider the 2 way range and range difference error performance.

In order to derive quantitative performance results, we shall assume the ranging system specifications listed below, though any changes from these values can be logically accommodated in the performance analysis that follows through the parametric formulation employed:

Orbital dynamics: $\dot{R} = 1$ m/s and $\ddot{R} = 1$ mm/s^2 for TDRS
$\dot{R} = 7$ km/s and $\ddot{R} = 10$ m/s^2 for USER

Tracking System Power budget:
$S/\Phi = 90$ dB-Hz for G.S./TDRS link
$S/\Phi = 55$-65 dB-Hz for TDRS/USER link
$S/\Phi = 40$ (low) or 60 (high) dB-Hz for USER/TDRS link
$S/\Phi = 80$ dB-Hz for TDRS/G.S. link

These specifications are representative of various TDRS system applications being studied and developed at GSFC when multipath and RFI are ignored; e.g., the ATS/NIMBUS and ATS/GEOS tracking experiments or the Geopause/Earth-Harmonic system development are current NASA programs that can be accomodated by these specifications. The basic characteristics are predominating USER orbital dynamics in the TDRS vs USER relative motion, plus predominating low SNR conditions in the TDRS/USER and USER/TDRS links.

2. SYSTEM DESCRIPTION

The system configuration and ranging signal propagation is illustrated in Figure 1 for 2-way and 1-way ranging. One or more TDRS's at synchronous altitudes are used to relay communication or tracking signals between a set of synchronized ground stations (G.S.) and a low-altitude USER spacecraft. The ground stations may be separated or co-located but their reference frequencies must be synchronized. A K-band signal will be employed for GS/TDRS communications and a VHF signal for USER/TDRS communications.

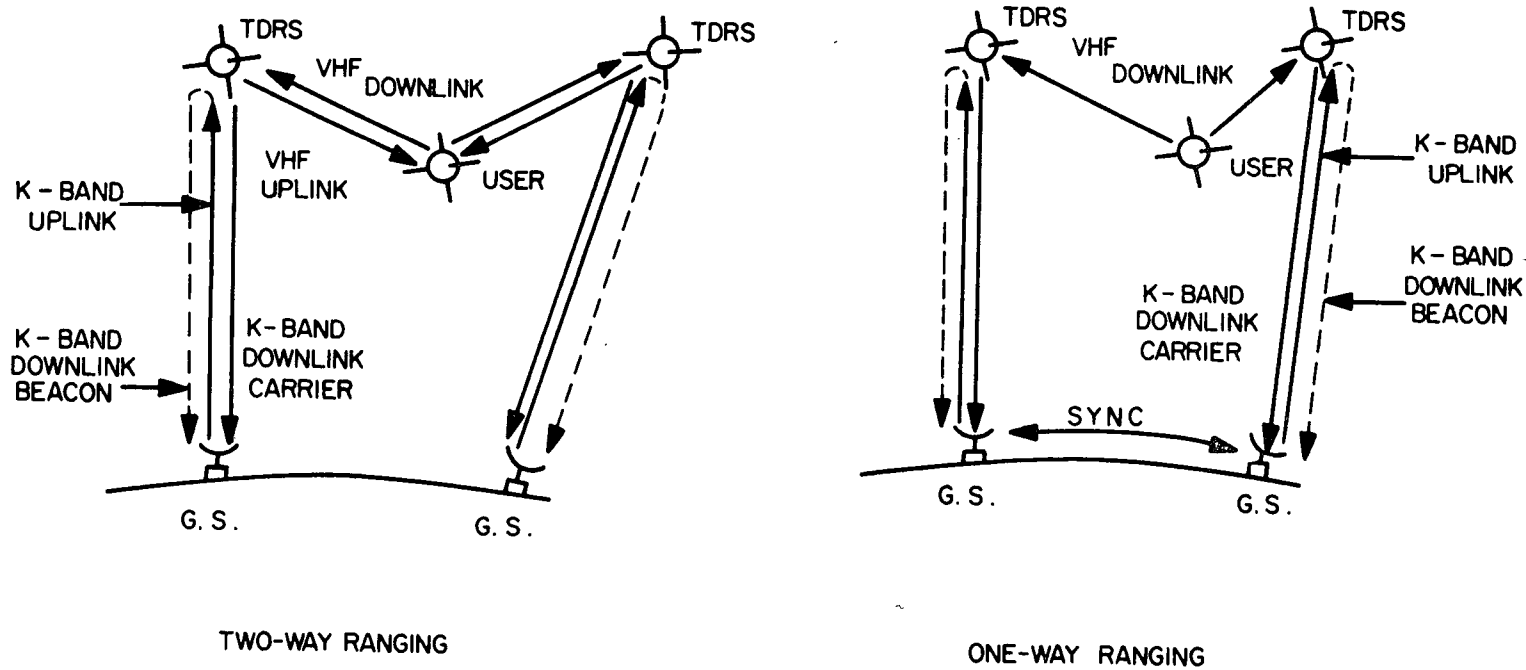

Figure 1. Ranging System Propagation Paths

In 2-way ranging systems, the ranging signals originate at ground and propagate through the G.S./TDRS/USER/TDRS/G.S. round-trip path so that the signal received at each ground station can be processed to provide 2-way range and/or 2-way range rate data. In 1-way ranging systems, the ranging signal originates at the USER spacecraft and propagates through the USER/TDRS/G.S. return link path. The signal received at each ground station can now only yield 1-way range rate data. When two TDRS's are employed two signals received at synchronized ground stations can be processed to provide 1-way range difference and/or 1-way range rate difference data as well as 1-way range rates. When both such 1-way signals are available, the two ground receivers have the option of independently extracting the ranging signals and then combining them to generate the range difference or range rate difference data, or the option of combining the received signals prior to extracting the tracking data from a composite signal. If the TDRS/USER geometry is such that only one TDRS maintains contact through certain time intervals, then the tracking data available is limited to 1-way range rate during those intervals, thus the former option of independent signal extractions is proposed for 1-way ranging.

In all cases, the TDRS's are assumed to be phase-locked to the K-band signal generated at the ground transmitter, and the TDRS loop VCO's are used to derive both the VHF TDRS/USER forward link carrier (which carries no tracking data in 1-way ranging) as well as the frequency references employed to translate the VHF USER/TDRS return link carrier to K-band for TDRS to ground relay purposes. Hence the TDRS's act as coherent transponders for the G.S./TDRS/USER forward link relay and as incoherent transponders for the USER/TDRS/G.S. return link. The term "pseudo-coherent transponder" has been used to designate such TDRS processing. This system unavoidably adds a scaled version of the G.S./TDRS uplink doppler to the USER/TDRS/G.S. return carrier (in non real time due to the TDRS/USER/TDRS propagation delay) as illustrated schematically in Figure 2. The inclusion of a direct K-band G.S./TDRS/G.S. beacon turnaround signal, also derived from the TDRS loop VCO's for doppler compensation or TDRS tracking purposes, becomes a natural consideration as indicated by the dashed lines in figure 1.

In 1-way ranging, the USER originates a VHF signal from an existing USER L.O. As such the signal is not related to the G.S./TDRS/USER forward link signal which contains communication and command but no ranging components. In 2-way ranging, the USER return link carrier will be assumed to be that of either a coherent or a GRARR (Goddard Range and Range Rate) type transponder as illustrated schematically in Figure 3. The user coherent transponder phase-locks to the VHF TDRS/USER forward link carrier and the USER phase locked loop VCO is used to derive the VHF USER/TDRS return link carrier. The GRARR transponder utilizes an incoherent USER L.O. which both generates

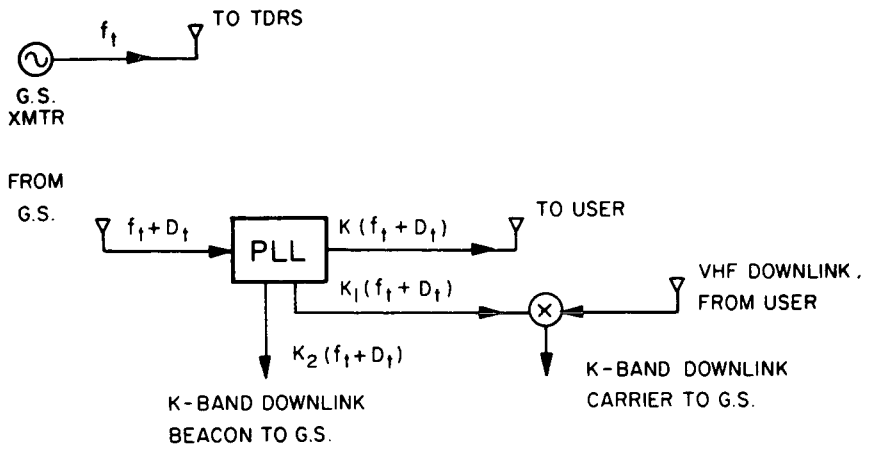

$$\left(K = \frac{\text{VHF UP}}{\text{K-BAND UP}},\ K_1 = \frac{\text{K-BAND CARRIER DOWN} \pm \text{VHF DOWN}}{\text{K-BAND UP}},\ K_2 = \frac{\text{K-BAND BEACON DOWN}}{\text{K-BAND UP}}\right)$$

Figure 2. TDRS Pseudo-Coherent XPDR Processing

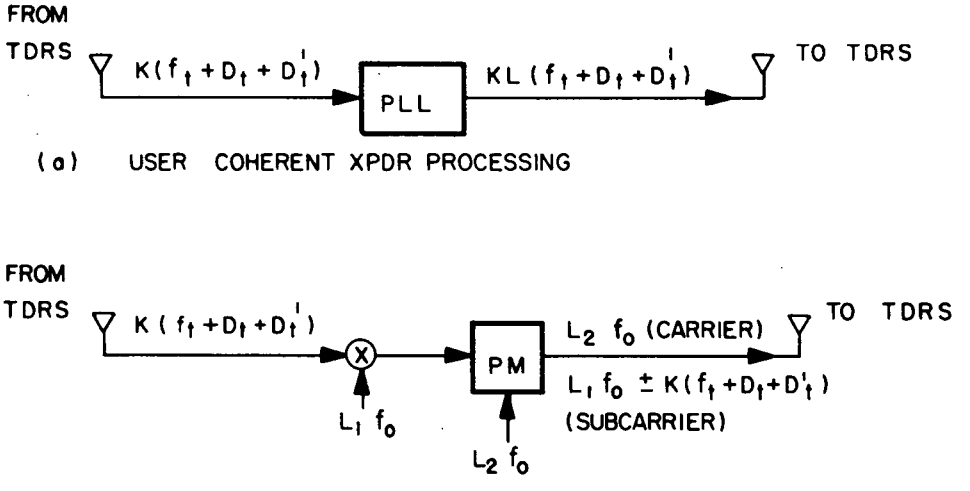

$$\left(KL = \frac{\text{VHF DOWN}}{\text{K-BAND UP}},\ L_2 = \frac{\text{VHF DOWN}}{\text{USER L.O.}}\right) \quad \text{(PRIMED VALUES REFER TO THE TDRS/USER EFFECT)}$$

Figure 3. User XPDR Processing Alternatives

the VHF USER/TDRS return link carrier and translates the VHF TDRS/USER forward link carrier to a return link subcarrier frequency. The inclusion of the USER L. O. in both carrier and subcarrier return link components eventually permits the compensation of the L.O. doppler and instability effects and the extraction of a 2-way coherent doppler signal at the ground station

3. DOPPLER SIGNAL EXTRACTION

The doppler signal propagation and extraction is illustrated in Figures 4 and 5 for 1-way and 2-way ranging respectively. If we assume that the ground receivers have no turnaround beacon signal available, the doppler reproduction potential is limited to a composite term of the form (second order doppler effects are neglected):

$\underbrace{(2K_1D_t)}$ $\pm$ $\underbrace{L(D_0+D_0')}$ for 1-way ranging

2-way K-band GS/TDRS/GS doppler effect — 1-way VHF USER/TDRS/GS doppler effect

$\underbrace{(2K_1D_t)}$ $\pm$ $\underbrace{2KL(D_t+D_t')}$ for 2-way ranging (coherent USER)

2-way K-band GS/TDRS/GS doppler effect — 2-way VHF GS/TDRS/USER/TDRS/GS doppler effect

$\underbrace{2\frac{L_1}{L_2}K_1D_t)}$ $\pm$ $\underbrace{2K(D_t+D_t')}$ for 2-way ranging (GRARR USER)

2-way K-band GS/TDRS/GS doppler effect — 2-way VHF GS/TDRS/USER/TDRS/GS doppler effect

The 2-way K-band TDRS doppler effect will always be added to the 1-way or 2-way VHF USER doppler effect. While the conditions $D_0 << D_0'$ and $D_t << D_t'$ will be met except at very small USER/TDRS relative velocities, the condition of small K-band G.S./TDRS/G.S. doppler is more restrictive since the TDRS doppler effect is emphasized by the K-band/VHF frequency ratio. The maximum doppler conditions correspond to a peak contribution of the order of 100 Hz from the first term of the equations and 3.5 kHz (1-way) or 7 kHz (2-way) from the second term, so that the composite doppler signal indeed reflects the user relative motion except at small USER/TDRS relative velocities.

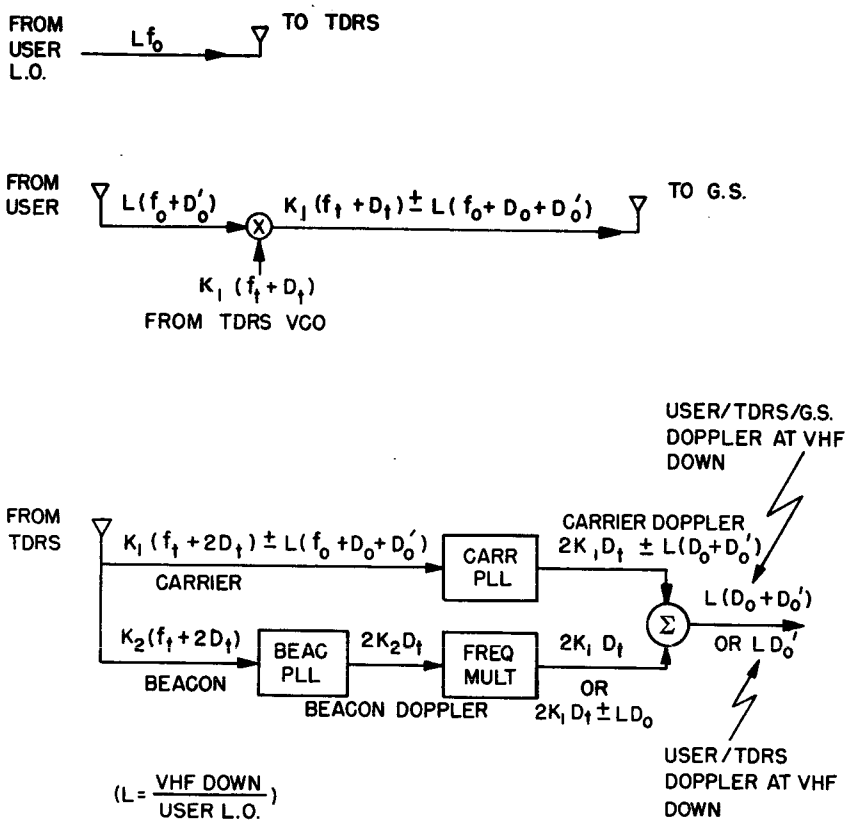

Figure 4. Doppler Signal Extraction in 1-Way Ranging

It should be understood that disregarding the first term in the expressions is tantamount to introducing a peak range rate bias error of (c/Lf_0) (100 Hz) $\approx$ 200 m/s for 1-way ranging and $(c/2KLf_t)$ (100 Hz) $\approx$ 100 m/s for 2-way ranging which even though small relative to the USER range rate yet may predominate over other error sources and effects when establishing tracking accuracy performance bounds in a given orbit determination program. The 2-way K-band G.S./TDRS/G.S. doppler can be compensated for by the inclusion of the turnaround beacon signal as illustrated in figure 1, in which case such bias error can be removed and the tracking performance improved. The beacon signal can also be used to compensate for all G.S./TDRS and TDRS/G.S. doppler contributions (i.e., remove all unprimed doppler terms) and yield only USER/TDRS and TDRS/USER doppler (primed) terms in the doppler signal extracted.

The advisability of using a turnaround beacon signal in 1-way ranging is further emphasized by oscillator noise compensation considerations. The beacon signal is of course derived from the TDRS VCO, and hence will contain the (TDRS-loop filtered) phase noise contributions in the reproduced G.S./TDRS uplink carrier. These oscillator phase noise contributions are then present in

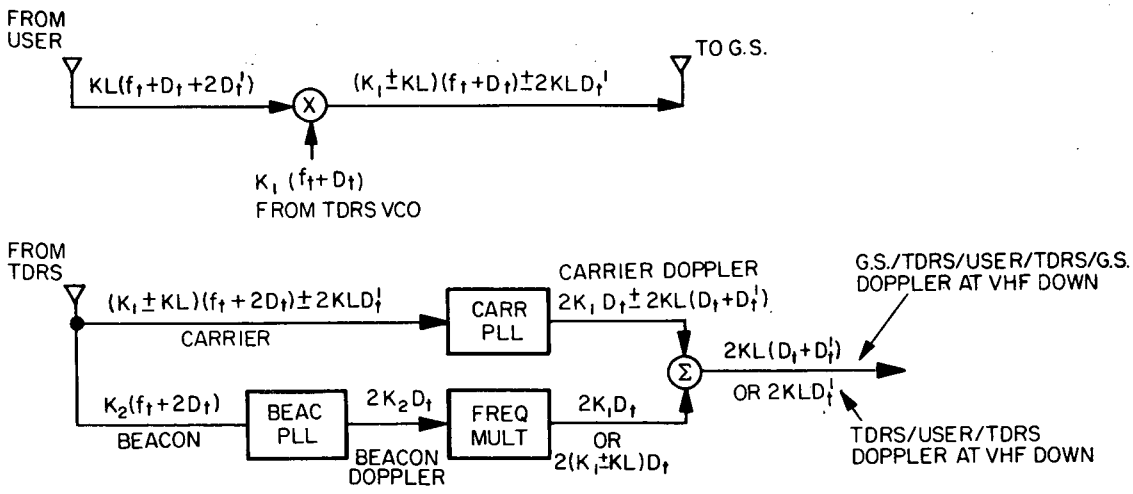

(a) DOPPLER EXTRACTION WITH COHERENT USER XPDR.

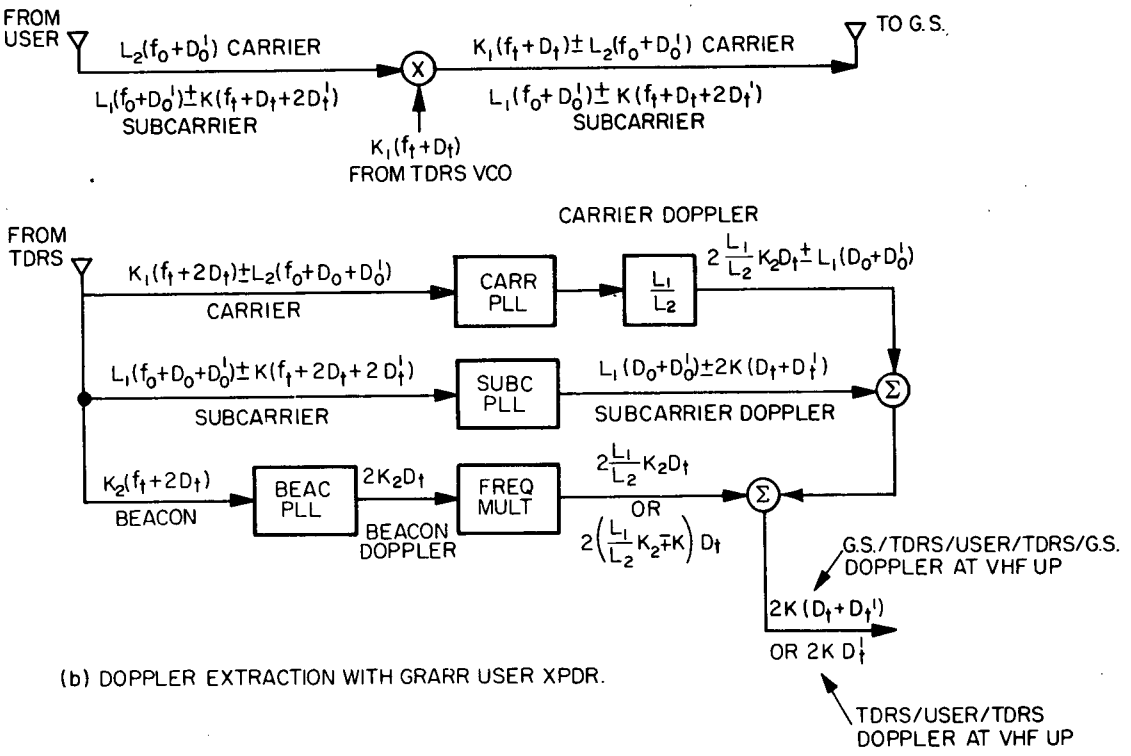

(b) DOPPLER EXTRACTION WITH GRARR USER XPDR.

Figure 5. Doppler Signal Extraction in 2-Way Ranging

both the TDRS/G.S. downlink carrier and beacon signals, and ideally differ only by the carrier/beacon frequency ratio. They can be eventually compensated for at the ground receiver when the beacon signal is referred to the carrier for doppler compensation. That is, provided that both downlink carrier and beacon signals exhibit negligible differential propagation delays (e.g., essentially same atmospheric effects) as well as equivalent filtering (e.g., same carrier and beacon loop receiver design) to preserve phase noise time-correlation. Moreover, the oscillator noise in the ground receiver RF reference used for IF conversion should be uncorrelated to the retransmitted oscillator noise in the received downlink signal (even though a common ground master oscillator is used to derive the transmitter carrier and the receiver references) due to the G.S./TDRS/G.S. propagation delay. Its K-band phase noise contribution should be accounted for in any system error analysis; i.e., the USER oscillator is expected to be more unstable than the ground master oscillator but the ground oscillator contributes K-band phase noise while USER contributes VHF phase noise. The use of a common receiver RF reference in both carrier and beacon extractions plus identical loop designs also provides K-band phase noise compensation of such local reference when the carrier and beacon signals are subtracted for doppler compensation purposes. The ground oscillator noise contribution will then be limited to the IF bias frequency accompanying the doppler signal thus making it negligible relative to the USER VHF oscillator noise contribution.

In summary, the inclusion of the turnaround beacon signal is recommended both for doppler and oscillator noise compensation in 1-way ranging, and of course can be used to provide 2-way G.S./TDRS/G.S. range rate data for TDRS tracking purposes. It should be emphasized that the oscillator noise compensation potential of the turnaround beacon approach is characteristic of the 1-way ranging system and may not be applicable in 2-way ranging. The oscillator noise in the TDRS/G.S. downlink carrier will still include the retransmitted G.S./TDRS uplink carrier and TDRS VCO effects in 2-way ranging, but they will also now exhibit the TDRS/USER/TDRS round-trip propagation delay (say, 0.25 sec) while the beacon signal will not propagate through this USER link. The downlink carrier and beacon signal received at ground will have time-uncorrelated phase noises even assuming an ideal coherent transponder at the USER (an effective width greater than 10 Hz is representative of oscillator phase noise spectral content so that effective correlation times smaller than the 0.25 sec propagation delays are characteristic). The TDRS/G.S. downlink carrier and beacon phase noise effects will then add mean-square wise rather than cancel each other, as a consequence of the additional TDRS/USER/TDRS propagation path, so that inclusion of the beacon signal provides doppler compensation at the expense of retransmitted oscillator noise enhancement.

It should also be noted that while the inclusion of the turnaround beacon approach in 1-way ranging does provide ground oscillator noise compensation making such error source small relative to the USER oscillator noise, it also doubles the mean-square contribution of the ground receiver VCO noise since the carrier and beacon loop VCO effects will be independent. Hence, the two basic oscillator noise processes to be considered in 1-way range rate systems are the USER VHF oscillator noise and the ground receiver carrier plus beacon VCO noises. These VCO noises will be filtered by the receiver loop error transfer function. This addition of carrier plus beacon receiver VCO noise is of course also present in 2-way ranging.

In Table 3 we have summarized the various oscillator noise contributions to the doppler signal extracted at the ground receiver, for 1-way and 2-way ranging with or without the turnaround beacon signal. The filtering introduced by the various tracking loop transfer functions is to be implicitly understood. The circled (no) entries identify those processes that are ideally compensated for by the beacon signal, and the extent to which these processes and their effects would have been commensurate with the remaining ones. The uncompensated processes require further investigation and perhaps even subsystem specification; e.g., the USER oscillator should be more unstable than the G.S. oscillator but it contributes VHF phase noise rather than K-band phase noise, so that the predominant effect is not a-priori evident particularly in high-accuracy systems where a good USER oscillator stability will be employed.

We thus propose the inclusion of the turnaround beacon as a desirable system conceptual design feature since:

(a) it provides TDRS tracking data,

(b) it provides G.S./TDRS/G.S. K-band doppler compensation in 1-way or 2-way ranging,

(c) it provides retransmitted G.S. and TDRS oscillator noise compensation in 1-way ranging,

(d) it provides G.S. receiver L.O. noise compensation at RF reducing such effects to IF in 1-way or 2-way ranging.

(e) it at most doubles the mean-square G.S. receiver VCO noise in 1-way or 2-way ranging.

TABLE 3
Oscillator Noise Contributions to Doppler Signal Extracted

Oscillator Noise Process	1-way ranging w/o beacon	2-way ranging w/o beacon	1-way ranging with beacon	2-way ranging with beacon
rexmtd GS/TDRS uplink carrier	yes (K-band)	yes (K-band)	(no)	yes (K-band)
rexmtd TDRS VCO	yes (K-band)	yes (K-band)	(no)	yes (K-band)
user L.O. or VCO	yes (VHF)	yes (VFH) if coherent USER	yes (VHF)	yes (VHF) if coherent USER
		no if GRARR USER		no if GRARR USER
GS rcvr RF reference	yes (K-band)	yes (K-band)	(no)	(no)
GS rcvr carrier (or subcarrier) loop VCO	yes	yes	yes	yes
GS rcvr beacon loop VCO	no	no	yes	yes
	no G.S./TDRS/G.S. K-band doppler compensation due to beacon absent		plus G.S./TDRS/G.S. K-band doppler compensation due to beacon present	

4. RANGE RATE ERROR ANALYSIS

The range rate data samples are assumed to be derived using conventional cycle-counting techniques on the doppler signal extracted at the ground receiver. The doppler signal consists of a bias frequency (f_b) plus the doppler extracted (Figures 4 and 5), so that the Number (N) of doppler plus bias cycles counted during a time T satisfies the relation $N = (f_b + f_d)\,T$ (Doppler rate and cycle quantization effects are neglected). The measurement of one parameter from the pair (N, T) while maintaining the other one fixed can thus be used to solve for the unknown doppler (f_d) and generate the corresponding range rate samples (k = 1, 2, 3. .) according to

$$\dot{r}_k = \frac{c}{L f_0} f_{d,k} \quad \text{for 1-way ranging} \tag{1a}$$

$$\dot{r}_k = \frac{c}{2 K L f_t} f_{d,k} \quad \text{for 2-way ranging (coherent USER)} \tag{1b}$$

$$\dot{r}_k = \frac{c}{2 K f_t} f_{d,k} \quad \text{for 2-way ranging (GRARR USER)} \tag{1c}$$

The range rate sample errors thus exhibit contributions from doppler measurement errors (e.g., phase noise or time jitter accompanying the bias plus doppler or introduced during the measurement operation) or from the use of incorrect values of the arithmetic constants used to convert doppler into range rate data (e.g., uncertainties in the velocity of light or long-term oscillator drifts). The doppler measurement itself may involve incorrect computation constants used to convert the measured parameter into doppler data (e.g., long-term bias frequency drifts) which of course must be accounted for in the error analysis. It should also be recognized that some error sources and effects are correlated so that they should be jointly rather individually evaluated to reflect such correlations; (e.g., a ground master oscillator drift will imply a different transmitter frequency $f_t \rightarrow f_t + \Delta f_t$ whose scaled doppler is being measured in 2-way ranging, as well as a different bias frequency $f_b \rightarrow f_b + \Delta f_b$ accompanying the doppler signal, plus a different frequency reference $f_r \rightarrow f_r + \Delta f_r$ being used as the time standard in the cycle counting process). The relation $\Delta f_t / f_t = \Delta f_b / f_b = \Delta f_r / f_r$ should be included in the error analysis in question.

The two range rate extractor realizations of interest are illustrated in Figures 6 and 7, where the measurement and arithmetic conversion operations

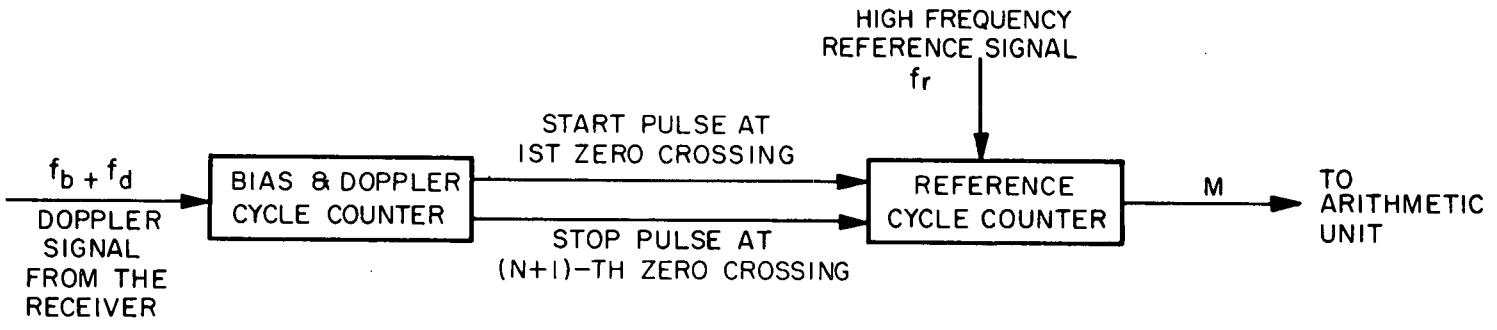

(a) MEASUREMENT UNIT

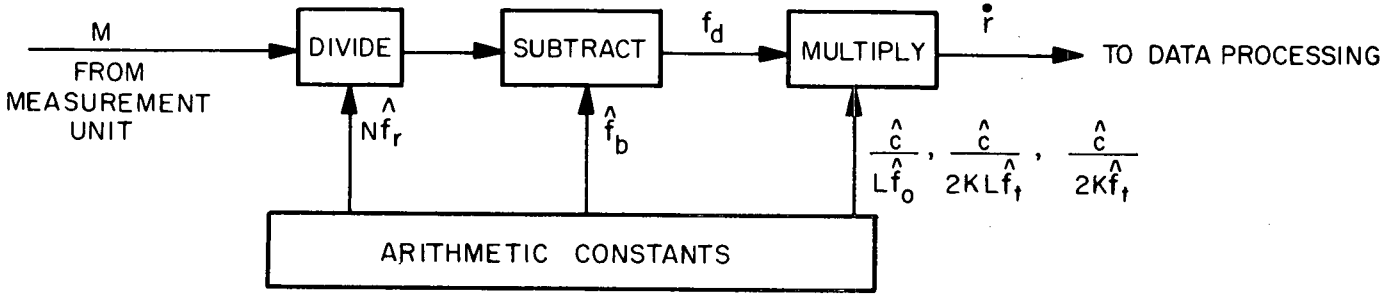

(b) ARITHMETIC UNIT

Figure 6. Range Rate Extraction: Fixed-N

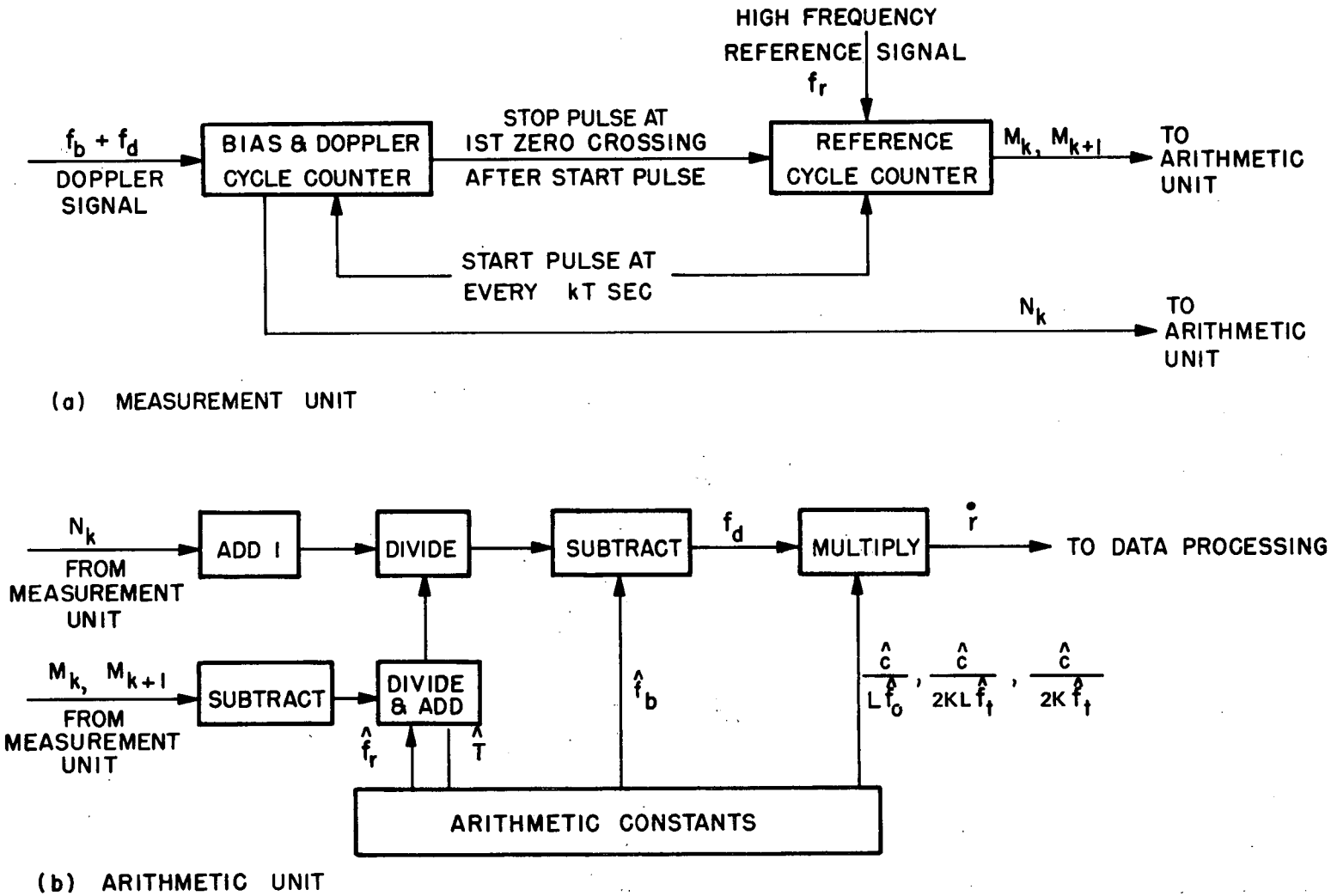

Figure 7. Range Rate Extraction: Fixed-T

are clearly identified. The hats are used to distinguish the arithmetic constants from their physical counterparts; e.g., the actual bias (f_b) and the reference (f_r) frequencies may differ from their nominal values ($\hat{f}_b$ and $\hat{f}_r$) used in the arithmetic unit due to oscillator drifts. In the fixed-N system the times $T_k = M_k/f_r$ corresponding to a preset number (N) of bias plus doppler cycles is measured in units quantized to a high-frequency reference period $1/f_r$ so that the number M_k of reference cycles is the actual parameter being measured and fed to the arithmetic unit. In the fixed-T system, the successive number of bias plus doppler cycles occurring in a time interval of preset duration T seconds consists of an integer number N_k, plus fractional quantization corrections to account for cycle fractions at the beginning and end of the counting period which are resolved from successive reference counts M_k as explained in Reference 3. The doppler effect measured in each case is given by

$$f_{d,k} = \frac{N}{M_k}\hat{f}_r - \hat{f}_b \quad \text{for fixed-N} \tag{2a}$$

$$f_{d,k} = \frac{N_k + 1}{(M_{k+1} - M_k) + \hat{T}\hat{f}_r}\hat{f}_r - \hat{f}_b \quad \text{for fixed-T} \tag{2b}$$

and the only cycle quantization errors present are those in the high-frequency reference counts M_k. The fixed-N exhibits dead zones of duration $U_k = T - T_k$ where the available doppler signal is not being processed (a constant range rate sample output rate 1/T is assumed), since the effective counting times T_k must be bounded by the sample separation T. This effect is absent in the fixed-T, which permits one to exploit error correlation between successive samples in the data smoothing filters preceding the orbital determination program, as explained in Reference 3.

Arithmetic and measurement error contributions to the range rate data thus extracted will now be evaluated. The following error sources and effects are considered:

(a) Uncertainty in the speed of light: (arithmetic) the conversion of the doppler measurement into range rate data uses this parameter so its uncertainties are reflected as range rate uncertainties.

(b) Oscillator drifts: (arithmetic) the long-term drifts of G.S. and USER oscillators result in the use of incorrect values for these constants so that range rate uncertainties are thus induced.

(c) Quantization noise: (measurement) the elapsed time is measured in units quantized to the reference period so that time (cycle) quantization effects are introduced and contribute doppler measurement errors.

(d) Time jitter: (measurement) the processing circuitry may add triggering pulse jitter which also introduces timing and doppler errors.

(e) Thermal noise: (measurement) the additive link noises become phase noises accompanying the doppler signal thus contributing phase jitter and doppler errors, plus retransmitted noises can cause signal suppression effects when nonlinearly processed at low SNR transponders.

(f) Oscillator noise: (measurement) the short-term instabilities of G.S. and USER L.O.'s and VCO's also introduce phase jitter and contribute doppler errors.

4.1 Arithmetic Errors

An uncertainty $|\Delta c|$ in the velocity of light represents a range rate uncertainty of

$$|\Delta \dot{R}| = \frac{|\Delta c|}{c} \dot{R} \quad \text{for 1-way or 2-way ranging} \tag{3}$$

so that a $|\Delta c|/c = 3 \times 10^{-7}$ implies a $|\Delta \dot{R}| = 2$ mm/s maximum. In 1-way ranging, a long-term (relative to the propagation time and doppler measurement duration) frequency drift (Δf_0) in the USER L.O. means that the measured doppler should be referred to the actual frequency L ($f_0 + \Delta f_0$) rather than the nominal Lf_0 value when converting the measured doppler into range rate data, thus introducing a net error (observed minus true value) of

$$\Delta \dot{R} = \frac{c\, f_d}{L\, f_0} - \frac{c\, f_d}{L\,(f_0 + \Delta f_0)} \approx \dot{R} \left(\frac{\Delta f_0}{f_0}\right) \quad \text{for 1-way ranging} \tag{4}$$

A long-term USER oscillator stability of 10^{-7} or better will be required to maintain this error within 1 mm/s and make it commensurate with the velocity of light uncertainty effect. In 2-way ranging, a USER L.O. will be present if a GRARR transponder is employed but a proportionate frequency drift will be induced in both carrier and subcarrier doppler contributions, and they will compensate in the doppler signal extraction process.

In 1-way ranging, a long-term drift (Δf_g) of the ground master oscillator will cause a proportionate drift (Δf_b) in the bias frequency accompanying the doppler plus bias signal. The doppler measurement is based on counting bias plus doppler cycles and arithmetically subtracting the nominal bias value to get doppler only, so any bias drift will be incorrectly preserved as a measured doppler and will induce a range rate error of

$$\Delta \dot{R} = \frac{c}{L f_0} \Delta f_d = -\frac{c}{L f_0} \Delta f_b = -\dot{R}\left(\frac{\Delta f_b}{f_d}\right) = -\dot{R}\left(\frac{f_b}{f_d}\right)\left(\frac{\Delta f_g}{f_g}\right) \tag{5}$$

However, this expression does not reflect the overall effect if the high-frequency reference used in the range rate extractor is also derived from the same master oscillator. For example, in the fixed-N, a simultaneous drift $f_r \rightarrow f_r + \Delta f_r$ and $f_b \rightarrow f_b + \Delta f_b$ would imply that the true doppler should be computed using the latter unknown values instead of the nominal ones, thus inducing a net range rate error of

$$\Delta \dot{R} = \frac{c}{L f_0} \Delta f_d = \frac{c}{L f_0}\left\{\left[\frac{N}{M} f_r - f_b\right] - \left[\frac{N}{M}(f_r + \Delta f_r) - (f_b + \Delta f_b)\right]\right\} = -\frac{c}{L f_0}\left(\frac{N}{M}\Delta f_r - \Delta f_b\right) \tag{6}$$

$$= -\frac{c}{L f_0}\left(\frac{N}{M} f_r - f_b\right)\left(\frac{\Delta f_g}{f_g}\right) \approx -\frac{c f_d}{L f_0}\left(\frac{\Delta f_g}{f_g}\right) = -\dot{R}\left(\frac{\Delta f_g}{f_g}\right) \text{ for 1-way ranging}$$

This is smaller in magnitude than the end result in (5) derived ignoring the reference drift correlation. The idea is that a positive bias drift causes more apparent doppler to be measured but time is counted faster due to the reference drift. A comparison of (4) and (6) shows that the USER and G.S. oscillator drift effects have the same functional dependence in 1-way ranging, so that USER drift effects should predominate since $\Delta f_0/f_0 >> \Delta f_b/f_b$. These results and conclusions are also applicable to the fixed-T extractor when one also assumes that the clock used to fix the T parameter is also derived from the same master oscillator so that $\Delta T/T = -\Delta f_g/f_g$; i.e.,

$$\Delta f_d = \left[\frac{(N+1)\, f_r}{(M) + T f_r} - f_b\right] - \left[\frac{(N+1)\,(f_r + \Delta f_r)}{(M) + (T + \Delta T)\,(f_r + \Delta f_r)} - (f_b + \Delta f_b)\right]$$

$$= \frac{(N+1)\, f_r}{(M) + T f_r}\left[\sum_{\substack{0 \\ \text{exclude} \\ m=n=0}}^{\infty}\sum_{0}^{\infty} (-1)^{m+n} \left(\frac{\Delta T}{T}\right)^m \left(\frac{\Delta f_r}{f_r}\right)^n\right]$$

$$- \frac{(N+1)\,\Delta f_r}{(M) + T f_r}\left[\sum_{\substack{0 \\ \text{include} \\ m=n=0}}^{\infty}\sum_{0}^{\infty} (-1)^{m+n} \left(\frac{\Delta T}{T}\right)^m \left(\frac{\Delta f_r}{f_r}\right)^n\right] + \Delta f_b \qquad (7)$$

$$\approx - \frac{(N+1)\, f_r}{(M) + T f_r}\underbrace{\left(\frac{\Delta T}{T} + \frac{\Delta f_r}{f_r}\right)}_{\text{zero}} - \frac{(N+1)\,\Delta f_r}{(M) + T f_r} + \Delta f_b = - f_d \left(\frac{\Delta f_g}{f_g}\right).$$

In 2-way ranging, the end result in (6) must now be extended to include the correlation between the transmitter uplink carrier drift (Δf_t) with the bias and reference frequency drifts. The net error in range rate for the case of a coherent USER transponder and a fixed-N extractor is given by:

$$\Delta \dot{R} = \frac{c}{2K f_t}\left[\frac{N f_r}{M} - f_b\right] - \frac{c}{2K(f_t + \Delta f_t)}\left[\frac{N}{M}(f_r + \Delta f_r) - (f_b + \Delta f_b)\right]$$

$$= \frac{c}{2K f_t}\left\{\left[\frac{N}{M} f_r - f_b\right]\cdot\left[\sum_{1}^{\infty} (-1)^n \left(\frac{\Delta f_t}{f_t}\right)^n\right] - \left[\frac{N}{M}\Delta f_r - \Delta f_b\right]\cdot\left[\sum_{0}^{\infty} (-1)^n \left(\frac{\Delta f_t}{f_t}\right)^n\right]\right\}$$

$$= \frac{c}{2K f_t}\left(\frac{N}{M} f_r - f_b\right)\cdot\left[\sum_{1}^{\infty} (-1)^n \left(\frac{\Delta f_g}{f_g}\right)^n - \sum_{0}^{\infty} (-1)^n \left(\frac{\Delta f_g}{f_g}\right)^{n+1}\right] \qquad (8)$$

$$= \frac{2c}{2K f_t}\left(\frac{N}{M} f_r - f_b\right)\left[\sum_{1}^{\infty} (-1)^n \left(\frac{\Delta f_g}{f_g}\right)^n\right] \approx - \frac{2c f_d}{2K f_t}\left(\frac{\Delta f_g}{f_g}\right) = - 2\dot{R}\left(\frac{\Delta f_g}{f_g}\right)$$

for 2-way ranging.

This shows that the ground oscillator drift effects are doubled in 2-way ranging relative to 1-way ranging. These results and conclusions are also applicable to a GRARR type USER transponder, or a fixed-T range rate extractor where $\Delta(Tf_r) = 0$ as previously discussed.

Table 4 summarizes the main results of the present section concerning arithmetic range rate error sources and effects in 1-way and 2-way ranging systems. In 1-way ranging, the USER and G.S. oscillator effects exhibit the same functional dependence. The percentage range rate error being given by the long-term stability so that USER oscillator effects should predominate as an error performance bound. In 2-way ranging, the USER oscillator contribution is absent while the G.S. oscillator contribution is doubled. It should be emphasized that the derivation of the G.S. oscillator effects has carefully accounted for the correlation existing between transmitter, bias and reference oscillator drifts in both fixed-N and fixed-T range rate extractors, so as to properly reflect the error contribution when a common master oscillator is employed at ground.

TABLE 4
Range Rate Arithmetic Errors

Error Source	1-way Ranging	2-way Ranging	Comments
Uncertainty in the Velocity of Light	$\frlvert\Delta \dot{R}\frrvert / \dot{R} = \frlvert\Delta c\frrvert / c$	$\frlvert\Delta \dot{R}\frrvert / \dot{R} = \frlvert\Delta c\frrvert / c$	$\lvert\Delta \dot{R}\rvert \approx 2$mm/s max for R = 7 km/s max
User Oscillator Long-Term Drift	$\Delta \dot{R} / \dot{R} \approx \Delta f_0 / f_0$	no effect	$\Delta \dot{R} < 1$mm/s requires 10^{-7} USER osc. stab. in 1-way ranging
G.S. Oscillator Long-Term Drift	$\Delta \dot{R} / \dot{R} \approx -\Delta f_g / f_g$	$\Delta \dot{R} / \dot{R} \approx -2 \Delta f_g / f_g$	$\Delta \dot{R} < 1$mm/s requires 10^{-7} G.S. osc. stab. in 1- or 2-way ranging

4.2 Measurement Errors: Quantization Noise and Time Jitter

In the fixed-N extractor, the time duration of the N doppler plus bias cycles is measured in units quantized to the high-frequency reference period $1/f_r$, so that quantization noise is introduced both at the beginning and end of the measurement operation (the start and stop pulses do not necessarily coincide with the

reference zero crossing). An unknown phase departure ($\Delta\theta$ rad) from the reference zero crossing at the start or stop pulse occurrence induces a measurement error $\Delta M = \Delta\theta/2\pi$ which of course is cancelled out if the same phase offset prevails for both pulses. A time-varying doppler effect will exclude this last possibility in general, and we can ssume the start and stop pulse phase offsets as independent random variables for all practical purposes.

Under these conditions, the resultant doppler measurement error induced is given by the expression

$$\Delta f_d = \left(\frac{N}{M} f_r - f_b\right) - \left(\frac{N}{M + \Delta M} f_r - f_b\right) \approx \frac{(f_b + f_d)^2}{N f_r} \Delta M \text{ Hz.} \qquad (9)$$

Its rms value corresponding to uniformly distributed independent phase offsets is given by

$$\sigma_{f_d} = \left(\frac{\sqrt{2}}{2\pi}\right) \frac{(f_b + f_d)^2}{N f_r} \sigma_{\Delta\theta} = \frac{(f_b + f_d)^2}{\sqrt{6}\, N f_r} = \frac{1}{\sqrt{6}\, T} \left(\frac{f_b + f_d}{f_r}\right) \text{Hz rms.} \qquad (10)$$

If we assume $f_b + f_d/f_r \approx 5 \times 10^{-3}$, which is representative of existing VHF tracking system design, and establish the measurement period to be reciprocal of the output data rate (i.e., neglect dead zone effects in the fixed-N extraction, which still yields commensurate error values for all practical purposes), then the previous expression reduces to $\sigma_{f_d} = 2 \times 10^{-3}/T$ Hz rms. This results in corresponding range rate errors of $\sigma_{\dot{R}} = 0.4/T$ cm/s rms for 1-way ranging and $\sigma_{\dot{R}} = 0.2/T$ cm/s rms for 2-way ranging. The point is that the quantization noise effect appears in the range rate extractor measurement operation regardless of whether 1-way or 2-way doppler is being counted, and a multiplier factor of 1/2 is introduced in the arithmetic operation (figures 6b and 7b) in 2-way ranging when converting doppler effect into range rate data using equations (1b) or (1c). The quantization error dependence on the data rate is illustrated in Table 5 assuming typical tracking system specifications ($f_b + f_d \approx 5 \times 10^{-3}\ f_r$).

In the fixed-T extractor, the reference counter will also exhibit a quantization effect at the stop pulse triggering, but not at the start pulse which is derived from the same master generating the reference signal. However, the measurement unit delivers two successive reference counts to the arithmetic unit so that again two phase offets need be considered in the analysis, and again they may be

TABLE 5
Range Rate Quantization Noise Errors

T (sec)	$\sigma_{\dot{R}}$ (2-way ranging)	$\sigma_{\dot{R}}$ (1-way ranging)
10	0.02 cm/s	0.04 cm/s
1	0.2 cm/s	0.4 cm/s
0.5	0.4 cm/s	0.8 cm/s
0.25	0.8 cm/s	1.6 cm/s
0.125	1.6 cm/s	3.2 cm/s

assumed to be independent random variables with a uniform distribution. The rms doppler measurement error induced is given by

$$\sigma_{f_d} = \left(\frac{\sqrt{2}}{2\pi}\right) \frac{(f_b + f_d)^2}{(N+1)\, f_r}\, \sigma_{\Delta\theta} \approx \frac{1}{\sqrt{6}\, T} \left(\frac{f_b + f_d}{f_r}\right) \text{Hz rms} \qquad (11)$$

so that the previous results are still applicable regardless of the extractor realization as expected.

The range rate error contributions of any start/stop time jitter caused by the electronic processing circuitry but absent in the signals themselves (e.g., axis-crossing or gating detector effects, but not oscillator noise) can also be accounted for in an analogous manner. For example, a 1 nanosec jitter represents a $2\pi \times 10^{-2}$ rad rms reference uncertainty which can be used as $\sigma_{\Delta\theta}$ (instead of $2\pi/\sqrt{12}$) in the previous formulation. Hence, time jitter conditions of 30 nanosec rms would be equivalent to quantization noise. Smaller values are actually observable in practice.

4.3 Measurement Errors: Thermal and Oscillator Noise in 1-Way Ranging

In 1-way ranging, the thermal noise processes added to the signal through the propagation links of Figure 1 eventually appear as additive phase noise in the doppler signal extracted at the ground receiver. The downlink additive thermal noise has contributions from both the USER/TDRS and TDRS/G.S. links, but the latter may be neglected assuming expected signal-to-noise density conditions. Also, the uplink G.S./TDRS additive noise becomes phase noise at the TDRS tracking loop and is scaled and retransmitted as such to ground when

side-stepping the USER signal at the TDRS for ground relay purposes. This retransmitted phase noise is also negligible relative to the downlink USER/TDRS thermal noise effect due to the high uplink G.S./TDRS signal-to-noise density conditions (even assuming the TDRS loop bandwidth to be somewhat wider than tracking requirements to permit unaided signal acquisition at the TDRS). Of course, the inclusion of the turnaround beacon compensation would introduce further retransmitted and received thermal noise processes in general uncorrelated to their carrier signal counterparts due to different spectral occupancy, but again their effects should be negligible relative to the downlink USER/TDRS thermal noise contribution with its predominant noise-to-signal density.

The rms one-way doppler and range rate errors may be evaluated from the expression

$$\sigma_{\dot{R}} = \frac{c}{L f_0} \sigma_D = \frac{c}{L f_0} \sigma_{\Delta\theta/2\pi T} = \frac{\sqrt{2}c}{2\pi L f_0 T} [R_\phi(0) - R_\phi(T)]^{1/2} \qquad (12)$$

where $\Delta\phi = \phi(T) - \phi(0)$, T is the doppler counting time and $R_\phi(\cdot)$ is the phase noise autocorrelation function given by the inverse transform

$$R_\phi(t) = \int_{-\infty}^{\infty} \frac{\Phi}{2S_c} |H_\ell(j\omega)|^2 e^{j\omega t} \frac{d\omega}{2\pi} \qquad (13)$$

where Φ/S_c is the noise-to-carrier density and $H_\ell(s)$ is the receiver loop transfer function. If the loop bandwidth is wider than the data sample rate (as is often the case) then $|R_\phi(T)| << R_\phi(0)$ and the one-way rms error expression reduces to

$$\sigma_{\dot{R}} = \frac{c}{L f_0} \sigma_D = \frac{c}{2\pi L f_0 T} (SNR)_\ell^{-1/2} \qquad (14)$$

where

$$(SNR)_\ell = \frac{S_c}{\Phi B_n} \quad \text{and} \quad B_n = \int_{-\infty}^{\infty} |H_\ell(j\omega)|^2 \frac{d\omega}{2\pi}$$

is the loop bandwidth assuming $H_\ell(0) = 1$.

A lower bound on the loop bandwidth is established from phase dynamic tracking requirements (doppler rates, short-term oscillator instabilities). If we assume a conventional 2nd-order loop design with a damping factor of $1/\sqrt{2}$ for the receiver loop, the doppler rate tracking error will be given by

$$\phi_e \text{ (doppler rate)} = \frac{405\,\dot{D}}{B_n^2} \text{ deg} \tag{15}$$

and since the predominant doppler rate contribution is $L\dot{D}_0' = 5$ Hz/s maximum ($\ddot{R} = 10$ m/s^2) then a loop bandwidth $B_n > 15 - 45$ Hz is required to maintain the locking error below 1-10 deg, with the wider bandwidth resulting in the tighter bound. The bandwidth constraint due to the short-term instabilities of the USER L.O. is in turn accounted for by representing the power spectral density of the oscillator phase noise in the parametric form

$$S_\phi(\omega) = \frac{A}{\omega^3} + \frac{B}{\omega^2} + \frac{C}{\omega} + D \tag{16}$$

where the constants depend on the type and quality of the oscillator in question. The rms locking error contribution is then evaluated for a given loop transfer function from the expression

$$\phi_e \text{ (osc noise)} = \left[\int_{-\infty}^{\infty} S_\phi(\omega)\,|1 - H_\ell(j\omega)|^2\,\frac{d\omega}{2\pi}\right]^{1/2} \text{ rad rms} \tag{17}$$

The A and B terms have been found to predominate for spacecraft oscillators when 2nd-order loops having a damping factor $1/\sqrt{2}$ and $B_n < 100$ Hz are employed, with $A = 1/450$ and $B = 10^{-3}/225$ representing typical one-sided VHF spectral characteristics.[4] Under these conditions, the approximation

$$\phi_e \text{ (USER L. O.)} \approx \left(\frac{9A}{8B_n^2} + \frac{\sqrt{2}B}{B_n}\right)^{1/2} = \frac{1}{20B_n}\sqrt{1 + \frac{B_n}{400}} \text{ rad rms for } B_n < 100 \text{ Hz} \tag{18}$$

has been found to be effective, so that $3 < B_n < 100$ Hz is sufficient to maintain this locking error within 1 deg rms. The doppler rate bound thus predominates

over the USER oscillator noise bound when typical spectral parameters are assumed for the latter.

When the turnaround beacon is employed in 1-way ranging, the retransmitted G.S./TDRS carrier and TDRS VCO jitter are compensated for, and the G.S. receiver L.O. jitter is scaled to the bias frequency (f_b) so that it should be negligible relative to the USER oscillator noise effect as an error performance bound. There remains the G.S. receiver VCO jitter effects of the carrier and beacon tracking loops, and their error magnitudes depend on the effective VCO operating frequency (including any frequency multipliers involved). This effective frequency need not be at K-band (as in the TDRS loop) due to the IF conversion with the receiver RF L.O. references. There is a rather limited amount of data available concerning VCO spectral parameter values; e.g., a 10 MHz VCO has been characterized with $A \approx 10$ and $B \approx 10^{-5}$ one-sided[5], in which case the locking error would be $3/B_n$ rad rms for 2nd-order loops having $B_n < 100$ Hz, so that $60 < B_n < 100$ Hz would be required to maintain a 3 deg rms error. However, existing NASA tracking systems have been specified with VCO locking errors within 3 deg rms for B_n as low as 10 Hz, and their 3rd-order loop realizations claim to essentially meet these specifications at VCO operating frequencies higher than 10 MHz.[6,7] On the basis of these systems and the analysis presented thus far we shall assume $B_n = 50$ Hz should be sufficiently wide to accommodate doppler rate, USER L.O. and G.S. receiver VCO locking errors.

The thermal noise error of (14) can now be evaluated using the 40/60 dB-Hz (low/high) power budget established in Section 1, though it should be understood that this SNR may not be fully applicable to the range rate signal due to the possible presence of carrier phase modulation for telemetry data or range measurement data. The corresponding (low/high) loop SNR and max/min) thermal noise locking errors for the two conditions of no carrier supression (no modulation) and 3.5 dB carrier supression (e.g., a 1.2 rad PM sidetone) using $B_n = 50$ Hz are then

	Unmodulated Carrier	Modulated Carrier
$(SNR)_\ell$	23/43 dB-Hz	19.5/39.5 dB-Hz
σ_n	2.8/0.28 deg rms	4.3/0.43 deg rms

which are adequate for locking purposes. The corresponding range rate errors due to thermal noise are shown in Table 6 as a function of output data rate 1/T. The use of higher data rates would violate the $B_n T >> 1$ condition required to neglect the $R_\phi(T)$ contribution to $\sigma_{\dot{R}}$ in (12). A detailed characterization of the phase noise correlation introduced by the tracking loop filtering would then be required for quantitative results.

TABLE 6
Range Rate Thermal Noise Errors (1-Way Ranging)

T (sec)	$\sigma_{\dot{R}}$ (unmodulated carrier)	$\sigma_{\dot{R}}$ (modulated carrier)
10	0.22/0.022 cm/s	0.34/0.034 cm/s
1	2.2/0.22 cm/s	3.4/0.34 cm/s
0.5	4.4/0.44 cm/s	6.8/0.68 cm/s
0.25	8.8/0.88 cm/s	13.6/1.36 cm/s
0.125	17.6/1.76 cm/s	27.2/2.72 cm/s

The effect of USER short-term oscillator instabilities in 1-way ranging can next be evaluated from the expression

$$\sigma_{\dot{R}} = \frac{c}{L f_0}\,\sigma_D = \frac{c}{L f_0}\,\sigma_{\left(\frac{\Delta\phi}{2\pi T}\right)} = \frac{\sqrt{2}\,c}{2\pi L f_0 T}\left[R_\phi(0) - R_\phi(T)\right]^{1/2}$$

$$= \frac{c}{2\pi L f_0}\left[\int_{-\infty}^{\infty} S_{\dot{\phi}}(\omega)\,|H_\ell(j\omega)|^2\left(\frac{\sin \omega T/2}{\omega T/2}\right)^2 \frac{d\omega}{2\pi}\right]^{1/2} \qquad (19)$$

where $S_{\dot{\phi}}(\omega) = \omega^2 S_\phi(\omega)$ is the power spectral density of the oscillator frequency jitter. We will assume that an ideal loop reproduction takes place under the small locking error conditions. If we also assume a predominant B-term in the spectral decomposition (equation 16), then the previous expression reduces to

$$\sigma_{\dot{R}} = \frac{c}{L f_0}\,\sigma_D = \frac{c}{2\pi L f_0}\left(\frac{2B}{T}\right)^{1/2} \qquad (20)$$

The USER L.O. contribution may be evaluated assuming the typical spectral parameter $B = 10^{-5}$ for the spacecraft VHF oscillator noise as

$$\sigma_{\dot{R}}\,(\text{USER Osc noise}) \approx \frac{1}{10\sqrt{T}}\ \text{cm/s rms} \qquad (21)$$

TABLE 7
Range Rate USER L.O. Noise Errors (1-Way Ranging)

T (sec)	$\sigma_{\dot{R}}$(USER L.O.)
10	0.03 cm/s
1	0.10 cm/s
0.5	0.14 cm/s
0.25	0.20 cm/s
0.125	0.28 cm/s

A comparison of the thermal noise (Table 6) with USER L.O. noise (Table 7) contributions to the one-way range rate error illustrates that the former predominates at the low (40 dB-Hz) power budget. For the high (60 dB-Hz) power budget, both error contributions will be commensurate at low output data rates, while thermal noise effects will again predominate at the high data rates. This results from the 1/T (thermal noise) vs $1/\sqrt{T}$ (oscillator noise) range rate error dependence. It should be noted that the thermal noise error is dependent on the loop noise bandwidth, while the oscillator noise error is independent of noise bandwidth, when its spectral B-term effect predominates.

Now considering G.S. receiver VCO noise, expression (19) must be modified by replacing $H_\ell(\omega)$ with $1 - H_\ell(\omega)$ to account for the loop effect, and by inserting a $\sqrt{2}$ rms multiplier, to account for the carrier plus beacon loop contributions. The G.S.-VCO thus contributes a locking error jitter to the doppler signal extracted, whereas the USER L.O. contributes tracked oscillator jitter to the signal. Note though that an unstable VCO and a stable USER L.O. could still make these contributions equivalent. The lack of available quantitative information on VCO phase noise spectra prevents the general evaluation of VCO range rate error contributions. An approach often followed to bypass this problem is to assume the VCO phase noise contribution to the doppler signal at the beginning and end of a counting period to represent uncorrelated random variables. In which case the one-way range rate error is related to the VCO locking errors by the expression

$$\sigma_{\dot{R}} = \frac{c}{L f_0}\sigma_D = \frac{c}{L f_0}\sigma\left(\frac{\Delta\phi}{2\pi T}\right) = \frac{\sqrt{2}\,c}{2\pi L f_0 T}\sigma_\phi = \frac{45}{T}\sigma_\phi \text{ cm/s} \qquad (22)$$

where σ_ϕ is the (carrier plus beacon) rms VCO locking error in radians. Under these conditions, a 1 deg rms locking error per loop would yield $\sigma_{\dot{R}} \approx 1/T$ cm/s. The VCO range rate error contribution would predominate over the USER L.O. effects previously evaluated, plus be equivalent to the thermal noise effects for the low power budget case, and would also predominate for the high power budget case.

It should be emphasized that these VCO results depend on the validity of their phase noise contributions to $\phi(0)$ and $\phi(T)$ being uncorrelated random variables. This is particularly evident by the $1/T$ functional dependence in (22), which is the same dependence exhibited by quantization (10) and thermal (14) noise errors, while the L.O. noise effects (20) exhibit a $1/\sqrt{T}$ functional dependence. The L.O. and VCO noise effects do not exhibit the same dependence, since the former is lowpass filtered by $H_\ell(j\omega)$ while the latter is highpass filtered by $1 - H_\ell(j\omega)$. The effective correlation time of the VCO locking error process and its loop design dependence is not well known at present which makes it difficult to analytically support the uncorrelation assumption.

Finally, it should be noted that the assumption of a predominate B-term in the spectral decomposition of the L.O. noise employed in evaluating the integral of (19) should be verified for a given application. The approach employed in this paper and the $1/\sqrt{T}$ dependence of the range rate error are characteristic of a "random walk" on the phase caused by thermal and shot noise perturbations. This dependence may not be valid if other oscillator perturbations predominate. As an example, low pass filtered additive noise phase modulation can result in a $1/\sqrt{T}$ or $1/T$ factor depending upon the filter transfer and cutoff characteristics.

4.4 Measurement Errors: Thermal and Oscillator Noise in 2-Way Ranging

In 2-way ranging, the USER/TDRS return link thermal noise should still predominate over the TDRS/G.S. and G.S./TDRS link noises as previously stated for 1-way ranging, but now the TDRS/USER forward link thermal noise effects must be examined since this is not necessarily a high SNR link. The ultimate effects of a moderate-to-low SNR in the TDRS/USER link also depend on the specific signal processing taking place at the USER transponder. For example, the inclusion of a limiter preceding the PLL in a coherent USER or the PM operation in a GRARR USER is a desirable process to smooth the signal level fluctuations with varying TDRS/USER range. In a coherent USER, the limiter effect alters the effective loop SNR and retransmitted thermal phase noise. A low USER/TDRS link power budget, relative to the TDRS/USER link power budget, may make such retransmitted phase noise small relative to the USER/TDRS thermal noise when considering the USER/TDRS phase noise effects upon G.S.

receiver tracking loops. In a GRARR USER, the limiter effect alters the modulation SNR fed to the phase modulator and causes both subcarrier signal suppression and increased retransmitted PM noise; again this noise may be small relative to the USER/TDRS link noise. The subcarrier signal suppression may still be significant and attenuate the USER/TDRS subcarrier power level, and essentially emphasize the locking errors due to the subcarrier noise and the range rate error contributions at the G.S. receiver.[3,8] In summary, both a coherent and GRARR USER could yield negligible retransmitted noise in 2-way ranging, and a GRARR USER could exhibit a significant subcarrier suppression and thermal noise degradation in the doppler signal and range rate data extracted.

The rms range rate errors due to thermal noise in 2-way ranging with a coherent USER are given by (12) and (14), except that Lf_0 is now replaced by $2KLf_t$ as indicated in (1b). The 2-way doppler rate increases by a factor of 2 relative to the 1-way doppler rate. As a result of this the G.S. receiver loop bandwidth requirement increases by a $\sqrt{2}$ factor, as a consequence of the B_n^2 functional dependence in (15). The L.O. noise is now due to the K-band retransmitted uplink carrier, so that if we assume its phase jitter is tracked by the TDRS and USER loops, then the expression (18) is valid except that different A and B values should be used to reflect ground standard instabilities at K-band (rather than the spacecraft VHF L.O.). The literature suggests $A = 1.5 \times 10^{-2}$ and $B = 2.4 \times 10^{-7}$ for a K-band standard[5], which results in a $1/8B_n$ rad rms error. A $7 < B_n < 100$ Hz would maintain such error within 1 deg rms. Under these conditions, the doppler rate predominates over the L.O. noise as in 1-way ranging. The G.S. receiver VCO noise in the loop bandwidth previously discussed in 1-way ranging must now be supplemented with the retransmitted TDRS and USER VCO effects in 2-way ranging for a coherent USER. The retransmitted TDRS effects will prevail since the TDRS VCO operates at K-band while the USER VCO operates at VHF, and the TDRS loop will be narrower than the USER loop from doppler dynamics considerations. The G.S. receiver loop will be wider than the TDRS loop, again based on doppler dynamics, so that we can assume that the retransmitted TDRS VCO locking error will be reproduced at the G.S.

Under these conditions, the assumed $B_n = 50$ Hz will still accommodate all locking errors in 2-way ranging. The rms range rate errors due to thermal noise would be 1/2 of those previously cited for 1-way ranging in Table 6, due to the 1/2 multiplier factor in (1b). The thermal noise contribution of the measured doppler is the same in 1-way or 2-way (coherent-USER) changing due to the predominant USER/TDRS return link noise, yet the doppler measurement is divided by 2 in 2-way ranging to get range rate data with a corresponding 6 dB improvement in thermal noise errors.

In the case of a GRARR USER, the expression (12) is valid with $Lf_0 \rightarrow 2Kf_t$, but (13) and (14) must be modified to reflect the presence of carrier plus subcarrier loop noise contributions; i.e.,

$$R_\phi(t) = \int_{-\infty}^{\infty} \left[\left(\frac{L_1}{L_2}\right)^2 \left(\frac{\Phi}{2S}\right)_c |H_{\ell,c}(j\omega)|^2 + \left(\frac{\Phi}{2S}\right)_{sc} |H_{\ell,sc}(j\omega)|^2 \right] e^{j\omega t} \frac{d\omega}{2\pi} \quad (23a)$$

$$R_\phi(0) = \left(\frac{L_1}{L_2}\right)^2 \left(\frac{\Phi}{2S}\right)_c B_{n,c} + \left(\frac{\Phi}{2S}\right)_{sc} B_{n,sc} = \frac{1}{2}\left[\frac{(L_1/L_2)^2}{(SNR)_{\ell,c}} + \frac{1}{(SNR)_{\ell,sc}}\right] \quad (23b)$$

If we again assume $|R_\phi(T)| << R_\phi(0)$, the rms range rate error due to thermal noise is given by

$$\sigma_{\dot{R}} = \frac{c}{2Kf_t}\sigma_D = \frac{c}{4\pi K f_t T}\left[\left(\frac{L_1}{L_2}\right)^2 (SNR)^{-1}_{\ell,c} + (SNR)^{-1}_{\ell,sc}\right]. \quad (24)$$

The carrier and subcarrier doppler dynamics are essentially the same under conventional GRARR transponder designs ($L_1/L_2 \approx 1$), in which case the carrier and subcarrier loops will exhibit the same lower limit on loop bandwidth selection. The subcarrier signal level will be lower than the carrier due to the modulation in the GRARR transponder, and perhaps show a further degradation due to the limiter suppression effect if the USER operates at moderate-to-low input SNR's. In turn, the subcarrier PM sidebands fold coherently at the G.S. receiver, thus introducing a 3 dB improvement in the subcarrier loop SNR. The development of quantitative results thus requires numerical assumptions regarding uplink or downlink modulation indices and USER input SNR conditions for a GRARR USER transponder.

If we assume typical GRARR tracking system design parameters (e.g., a 1.2 radian PM'ed uplink carrier and 0-5 dB USER input SNR), each downlink subcarrier sideband is 6-8 dB down from the modulated carrier and 11-13 dB down from the unmodulated carrier power, so that the subcarrier noise will govern the range rate error contribution. The assumption of $B_n = 50$ Hz again accounts for all doppler rates, G.S. retransmitted and USER L.O. effects, and TDRS and G.S. VCO effects in the G.S. carrier/subcarrier tracking loops. A subcarrier loop SNR of 13-15 dB for the 40 dB-Hz low budget and 33-35 dB for the 60 dB-Hz high budget will exist (including the 3 dB folding improvement). This represents a 4.5-6.5 dB SNR degradation relative to 2-way ranging with a

coherent USER, so that the 1-way ranging performance is equivalent to that of 2-way ranging when considering a GRARR USER transponder operating at low SNR.

The L.O. noise contribution to range rate errors in 2-way ranging is due to the retransmitted G.S./TDRS uplink carrier, which appears on the carrier and beacon signals. This can not be compensated for due to the time delay introduced by the TDRS/USER/TDRS round-trip. The exclusion of the beacon does not reduce the L.O. noise contributions, since then the G.S. receiver RF L.O. instability would have to be considered. The development of (19)-(20) with Lf_D replaced by $\sqrt{2}\ KLf_t$ or $\sqrt{2}Kf_t$ is applicable, and the use of B (in equation 16) = 2.4×10^{-7} as the predominant spectral term for a K-band standard yields an rms error improvement of $\sqrt{2}\ (1/0.024)^{1/2} \approx 9$ over the results of (21) and Table 7. That is, the 2-way ranging contributes K-band L.O. noise while 1-way ranging contributes VHF L.O. noise, but this is more than compensated for by the highly-stable ground L.O. source utilized in 2-way ranging relative to the more unstable L.O. source in 1-way ranging.

The VCO noise contribution to range rate error in 2-way ranging requires consideration of G.S., TDRS and USER VCO's. The GRARR USER case does not employ a USER (VHF) VCO as is present in a coherent USER, but a G.S. subcarrier VCO exists with a GRARR USER and not with a coherent USER. The TDRS VCO noise contribution will no longer be compensated for by the beacon signal due to the additional TDRS/USER/TDRS propagation delay and the time uncorrelation it introduces. If we assume the uncorrelated phase noise developed in (22) with $Lf_0 \rightarrow 2KLf_t$ or $2Kf_t$ plus the same rms locking error in all loops in question, the 2-way ranging VCO noise contribution will exceed the 1-way ranging case by an rms factor of 2 due to the additional TDRS and G.S. subcarrier loops (GRARR USER) or TDRS and USER loops (coherent USER). The validity of identical locking error conditions must however be verified in a given application due to the different loop designs involved (e.g., the TDRS VCO operates at K-band, the USER VCO at VHF and the G.S. VCO's at IF). The TDRS loop bandwidth may be much narrower than the others from doppler tracking considerations.

5. RANGE SIGNAL EXTRACTION

The 1-way and 2-way ranging systems are both capable of providing range rate data, and an error performance comparison was performed (Section 4). The 1-way ranging can provide range-difference data when two TDRS's are in simultaneous contact with the USER and G.S. The 2-way ranging systems can of course provide range data, and we shall illustrate their error performance capabilities. However a direct comparison will not establish the relative merits due to the different-type of data extracted. The performance evaluation of 1-way range-difference vs 2-way range data systems is reflected only after such data

has been processed and used with their respective orbital determination programs to establish orbital uncertainties.

We shall assume sidetone ranging techniques where the ranging event is the zero-crossing of a sinusoidal tone which is PM'ed on the carrier for transmission purposes. The carrier doppler is used to derive range rate data as previously analyzed, while the event propagation delay is used to derive range or range-difference data. The tone frequency (f_s) is assumed to be high enough to match existing VHF tracking system specification (say, 20 kHz), and the resolution of ambiguities through the inclusion of sequential lower frequency tones is implicitly assumed.

In 1-way ranging, the tones are generated at the USER from the same L.O. employed to produce the USER/TDRS VHF return link carrier, and the TDRS side-stepping operation of the PM downlink signal with a phase-locked replica of the G.S./TDRS uplink signal follows as before, except that two TDRS are now involved. The downlink signal propagation is summarized in Table 8, where the G.S. receiver processing is based on the independent extraction of the two downlink signals prior to their combination to yield the range-difference data. The K-band downlink carriers extracted at the G.S. receiver are used to product demodulate their respective tones which are then extracted by PLL's. The time-dependent phase terms in the formulation include all doppler dynamics, oscillator instabilities and thermal noise contributions to be identified in the discussion that follows. The effect of loop locking errors has not been made explicit in the formulation to simplify the notation. Carrier locking errors will produce AMattenuation of the tone sidebands ($\cos\phi$) but small or no SNR degradation will result if a proper carrier lock prevails.

In 2-way ranging, the tones are generated at the G.S. transmitter from the same master oscillator used to produce the G.S./TDRS K-band uplink carrier, and the TDRS coherently translates the PM signal to VHF for TDRS/USER transmission purposes. The USER has either a coherent transponder which coherently translates the PM signal to another VHF for USER/TDRS transmission purposes (possibly including tone detection and remodulation), or it has a GRARR transponder where the received spectrum becomes a return link PM subcarrier. The TDRS side-stepping and G.S. receiver carrier/subcarrier extraction follows as before, and the ranging tone is again product demodulated and phase compared at ground to provide the range data. We shall omit the 2-way coherent or GRARR ranging signal propagation formulation, since they are characteristic of various existing NASA tracking systems and are well documented elsewhere (ref. 6).

TABLE 8
1-Way Ranging Signal Propagation

USER XMTR

$$A_c \cos [\omega_c t + \theta_c (t)] \pm A_s \cos [(\omega_c \pm \omega_s) t + \theta_c (t) \pm \theta_s (t)]$$

TDRS REVR's

$$B_c \cos [\omega_c (t - T_1) + \theta_c (t - T_1)] \pm B_s \cos [(\omega_c \pm \omega_s)(t - T_1) + \theta_c (t - T_1) \pm \theta_s (t - T_1)]$$

and

$$B'_c \cos [\omega_c (t - T'_1) + \theta_c (t - T'_1)] \pm B'_s \cos [(\omega_c \pm \omega_s)(t - T'_1) + \theta_c (t - T'_1) \pm \theta_s (t - T'_1)]$$

TDRS VCO's

$$\cos [\omega_v t + \theta_v (t)]$$

and

$$\cos [\omega_v t + \theta'_v (t)]$$

TDRS XMTR's: $\omega_r = \omega_v - \omega_c$

$$C_c \cos [\omega_r t + \theta_v (t) - \theta_c (t - T_1) + \omega_c T_1] \pm C_s$$

$$\cos [(\omega_r \mp \omega_s) t + \theta_v (t) - \theta_c (t - T_1) \mp \theta_s (t - T_1) + (\omega_c \pm \omega_s) T_1]$$

and

$$C'_c \cos [\omega_r t + \theta'_v (t) - \theta_c (t - T'_1) + \omega_c T'_1] \pm C'_s$$

$$\cos [(\omega_r \mp \omega_s) t + \theta'_v (t) - \theta_c (t - T'_1) \mp \theta_s (t - T'_1) + (\omega_c \pm \omega_s) T'_1]$$

TABLE 8–(continued)

G.S. RCVR's

$$D_c \cos [\omega_r (t - T_2) + \theta_v (t - T_2) - \theta_c (t - T_1 - T_2) + \omega_c T_1] \pm D_s$$

$$\cos [(\omega_r \mp \omega_s)(t - T_2) + \theta_v (t - T_2)$$

$$- \theta_s (t - T_1 - T_2) \mp \theta_s (t - T_1 - T_2) + (\omega_c \pm \omega_s) T_1]$$

and

$$D_c' \cos [\omega_r (t - T_2') + \theta_v' (t - T_2') - \theta_c (t - T_1' - T_2') + \omega_c T_1'] \pm D_s'$$

$$\cos [(\omega_r \mp \omega_s)(t - T_2') + \theta_v' (t - T_2')$$

$$- \theta_c (t - T_1' - T_2') \mp \theta_s (t - T_1' - T_2') + (\omega_c \pm \omega_s) T_1']$$

CARR PLL's:

$$\omega_b = \omega_{\ell_0} - \omega_r$$

$$D_c \sin [\omega_b t + \theta_{\ell_0} (t) - \theta_v (t - T_2) + \theta_c (t - T_1 - T_2) + \omega_v T_2 - \omega_c (T_1 + T_2)]$$

and

$$D_c' \sin [\omega_b t + \theta_{\ell_0}' (t) - \theta_v' (t - T_2') + \theta_c (t - T_1' - T_2') + \omega_v T_2' - \omega_c (T_1' + T_2')]$$

TONE PLL's

$$2 D_s \cos [\omega_s t + \theta_s (t - T_1 - T_2) - \omega_s (T_1 + T_2)]$$

and

$$2 D_s \text{ cis } [\omega_s t + \theta_s (t - T_1' - T_2') - \omega_s (T_1' + T_2')]$$

Legend:
- ω_c = VHF downlink carrier frequency
- ω_s = ranging sidetone frequency
- ω_v = TDRS side-stepping reference from VCO's
- ω_r = K-band downlink carrier frequency
- ω_b = G.S. receiver IF bias frequency
- ω_{ℓ_0} = G.S. receiver RF L.O. frequency
- T_1 and T_1' = USER/TDRS propagation delay
- T_2 and T_2' = TDRS/G.S. propagation delay.

The range measured is obtained by counting the elapsed time between transmission and reception of the ranging event (tone zero crossing). We shall assume a $f_{c\ell} = 100$ MHz clock is used for counting purposes, which is representative of existing tracking system design. The range-difference measured is obtained by counting the elapsed time between the two receptions of the ranging event originated by the USER and relayed by the two TDRS. Hence the actual measured parameter in either case is an integer number $n_{c\ell}$ of clock cycles, and the range and range-difference data is obtained via the arithmetic computation

$$R = \frac{c}{2 f_{c\ell}} n_{c\ell} \quad \text{for range data} \tag{25a}$$

$$R_1 - R_2 = \frac{c}{f_{c\ell}} n_{c\ell} \quad \text{for range-difference data} \tag{25b}$$

It should be understood that the received tone in 1-way or 2-way ranging will not only carry the USER/TDRS or TDRS/USER/TDRS range information but also the TDRS/G.S. or G.S./TDRS/G.S. range information. We shall assume here that TDRS tracking signals are available to resolve the G.S./TDRS baseline range without any interfacing with the USER tracking operation so that independent TDRS and USER error analyses are applicable. The potential longer tracking time available for TDRS tracking in contrast to USER tracking should be exploited in the TDRS data processing and orbit determination program, and will tend to validate our assumption of independent TDRS and USER error performance evaluations.

6. RANGE AND RANGE-DIFFERENCE ERROR ANALYSIS

We shall now evaluate the arithmetic and measurement error contributions to the range and range-difference data thus extracted. The following error sources and effects are considered:

(a) Uncertainty in the speed of light: (arithmetic) the conversion of elapsed time into range or range-difference data uses this parameter in the computation so its uncertainties are reflected as tracking data uncertainties.

(b) Oscillator drifts: (arithmetic) the long-term drifts of the G.S. master oscillator results in the use of incorrect values of the clock frequency so that range or range-difference errors are thus induced.

(c) Dynamic locking errors: (measurement) the tracking loops introduce phase shifts when reproducing the tone doppler dynamics, which represent timing and ranging errors in the data extracted.

(d) Thermal noise: (measurement) the additive link noises become phase noise in the reproduced tone thus contributing phase jitter and ranging errors, plus retransmitted noises can cause signal suppression effects when nonlinearly processed at low SNR's.

(e) Oscillator noise: (measurement) the short-term instabilities of G.S. and USER L.O.'s and VCO's appear on the received tone and contribute timing and ranging errors.

(f) Quantization noise: (measurement) the elapsed time is measured in units quantized to the clock period so that time (cycle) quantization is introduced and contributes ranging errors.

(g) Time jitter: (measurement) the processing circuitry introduces time jitter in the elapsed time measurement which induces ranging errors.

6.1 Arithmetic Errors

An uncertainty $|\Delta c|$ in the velocity of light represents range and range-difference uncertainties of

$$|\Delta R| = \frac{|\Delta c|}{c} R \tag{26a}$$

$$|\Delta (R_1 - R_2)| = \frac{|\Delta c|}{c} (R_1 - R_2) \tag{26b}$$

so that a $|\Delta c|/c = 3 \times 10^{-7}$ implies a $|\Delta R| \approx$ 10-12 m and $|\Delta (R_1 - R_2)| \approx$ 2.5 m peak when the TDRS/USER range is the data being considered. The minimum range corresponds to the USER being colinear with a TDRS and the earth center, while a maximum range corresponds to the USER forming a right triangle with a TDRS and the earth center.

A long-term drift of the G.S. master oscillator in either ranging system means that the actual clock frequency ($f_{c\ell} + \Delta f_{c\ell}$) should be used as the arithmetic constant instead of its nominal value $f_{c\ell}$, thus introducing a net error of:

$$\Delta R = \frac{c\, n_{c\ell}}{2 f_{c\ell}} - \frac{c\, n_{c\ell}}{2 (f_{c\ell} + \Delta f_{c\ell})} \approx R \left(\frac{\Delta f_{c\ell}}{f_{c\ell}} \right) = R \left(\frac{\Delta f_g}{f_g} \right) \tag{27a}$$

$$\Delta (R_1 - R_2) = \frac{c\, n_{c\ell}}{f_{c\ell}} - \frac{c\, n_{c\ell}}{f_{c\ell} + \Delta f_{c\ell}} \approx (R_1 - R_2) \left(\frac{\Delta f_{c\ell}}{f_{c\ell}} \right) = (R_1 - R_2) \left(\frac{\Delta f_g}{f_g} \right) \tag{27b}$$

Thus a master oscillator stability of 3×10^{-7} is required to equal the velocity of light uncertainty effects.

The tone extraction loops at the G.S. receivers introduce dynamic lag errors when reproducing the tone doppler dynamics. A loop tracking error of $\Delta\theta$ radians corresponds to timing and ranging errors of

$$\Delta R = \frac{c}{2} (\Delta t) = \frac{c}{4 \pi f_s} (\Delta \theta) \quad \text{for range data} \tag{28a}$$

$$\Delta (R_1 - R_2) = c\, (\Delta t) = \frac{c}{2 \pi f_s} (\Delta \theta_1 - \Delta \theta_2) \quad \text{for range-difference data} \tag{28b}$$

We shall assume f_s = 20 kHz plus no rate-aiding* involved.

The phase errors due to an uncompensated tone doppler shift (D_s (Hz)) and doppler rate ($\dot{D}_s$ (Hz/s)) are respectively given by $360 D_s / K_\ell$ and $405 \dot{D}_s / B_n^2$ deg. assuming 2nd-order loops with a $1/\sqrt{2}$ damping factor where K_ℓ is the loop gain. The uncompensated 1-way doppler conditions are about 1 Hz and 0.7×10^{-3} Hz/s, so that negligible doppler shift errors are feasible with available high loop gains. The doppler rate error contributions are tabulated in Table 9 for

*Note: Rate-aiding implies that the carrier doppler is used to estimate and compensate the tone doppler dynamics within some margin prior to the tone loop extraction, so as to permit narrower tracking bandwidths and more additive noise rejection than would be possible otherwise. The compensation process is then reversed after the rate-aided tone is loop filtered so that the regular tone doppler dynamics are recovered but with a smaller thermal phase noise contribution from the tracking loop than would occur in the absence of rate-aiding.

TABLE 9
Dynamic Lag Ranging Errors

B_n	$\Delta\theta$ (2-way)	$\Delta\theta$(1-way)	ΔR	$\Delta(R_1 - R_2)$
1 Hz	0.57	0.28	11.8 m	23.6 m
5 Hz	0.023	0.011	0.47 m	0.94 m
25 Hz	0.00091	0.00045	0.029 m	0.038 m

typical tone loop bandwidths in the absence of rate-aiding. The locking errors are doubled in 2-way ranging due to the 2-way tone doppler rate to be tracked, yet this effect is equalized by the 1/2 multiplier indicated in (28). However, the peak 1-way range-difference errors are twice the peak range errors by considering the maximum opposite-sign doppler rate conditions that may prevail in the two USER/TDRS links.

A comparison of the systematic errors shows that long-term oscillator drifts can be neglected as an error source relative to the velocity of light uncertainty based upon state-of-the-art master oscillator stability. The dynamic lag errors will be commensurate with the velocity of light effects when the narrower tracking bandwidths are used for range data, and will predominate over the velocity of light effects when the narrower bandwidths are used for range-difference. The velocity of light uncertainty predominates over dynamic lag effects for both range and range-difference data at the wider bandwidths.

6.2 Measurement Errors

The formulation of (28) can also be used to evaluate random phase error contributions of thermal and oscillator noise processes. The thermal noise error in the range and range-difference data has an rms value specified in terms of the tone loop SNR by

$$\sigma_R = \frac{c}{4\pi f_s}\sigma_\theta = \frac{c}{4\sqrt{2}\pi f_s}(SNR)_\ell^{-1/2} \quad \text{for range data} \tag{29a}$$

$$\sigma_{R_1-R_2} = \frac{c}{2\pi f_s}\sigma_{\theta_1-\theta_2} = \frac{c}{2\pi f_s}\left[\frac{1}{2SNR_1} + \frac{1}{2SNR_2}\right]^{1/2} = \frac{c}{2\pi f_s}(SNR)_\ell^{-1/2} \quad \text{for range-difference data} \tag{29b}$$

where it is assumed that identical loop SNR's exist as a worst case condition (otherwise a maximum $\sqrt{2}$ range difference error reduction may exist).

In 1-way ranging the tone level and loop SNR's depend on the PM index at the USER transmitter; e.g., a 1.2 rad sidetone has each sideband 6 dB down from available power and the loop signal-to-noise density is 3 dB down from the power budget specification on account of the 3 dB sideband folding improvement. In 2-way ranging with a coherent USER, the same loop SNR will be applicable provided that TDRS/USER power budget is large relative to the USER/TDRS SNR so that retransmitted additive noise can be neglected. In 2-way ranging with a GRARR USER, the existence of moderately-to-low input SNR at the USER transponder will again cause tone signal suppression as discussed earlier for the subcarrier component. If we assume the numerical example previously considered, each downlink tone sideband would be 9-11 dB down from the modulated carrier and 14-16 dB down from the available power, and the loop signal-to-noise density is 8-10 dB down from the power budget specification on account of the 6 dB sideband folding improvement.

If we assume the same loop bandwidth in 1-way and 2-way ranging, the loop SNR's will be the same in 1-way and 2-way coherent-USER cases so that the rms range error will be smaller by a factor of $2\sqrt{2}$ relative to the rms range-difference error. However, the tone suppression present in 2-way GRARR-USER ranging would tend to compensate such factor as happened with the range rate data; e.g., the numerical example in question has the received GRARR-USER tone 5-7 dB down relative to the coherent-USER case which reduces the rms range error improvement to a factor of 1.25-1.55 relative to the rms range-difference error. In summary, the range data exhibits an 8.9 dB SNR improvement over the range-difference data if a coherent-USER is employed, but only a 1.9-3.9 dB improvement if a low SNR GRARR-USER is employed. The locking errors and corresponding range and range-difference errors are illustrated in Table 10 as a function of the loop bandwidths under consideration for the 40/60 dB-Hz power budget options.

TABLE 10
Thermal Noise Ranging Errors

B_n	σ_θ (2-way coherent)	σ_θ (2-way GRARR)	σ_θ (1-way)	σ_R (2-way coherent)	σ_R (2-way GRARR)	$\sigma_{R_1-R_2}$ (1-way)
1 Hz	0.57/0.057°	1.14/0.114°	0.57/0.057°	12/1.2 m	24/2.4 m	33.5/3.4 m
5 Hz	1.3/0.13°	2.6/0.26°	1.3/0.13°	27/2.7 m	54/5.4 m	75.5/7.6 m
25 Hz	2.8/0.28°	5.7/0.57°	2.8/0.28°	58/5.8 m	116/16 m	162/16.2 m

The short-term jitter of the G.S. and USER oscillators that generate the ranging tone in 2-way and 1-way ranging respectively will appear on the tone scaled to its frequency and will be tracked by the G.S. tone loop. In 2-way ranging, the tone jitter at transmission and reception of the ranging event (time zero crossing) represent uncorrelated random variables due to the propagation time delay, so their effects add mean-square wise when evaluating range errors. A 3 nanosec rms time jitter on each zero crossing will induce an error of $\sigma_R = (c/2)\sigma_{\Delta t} = (\sqrt{2}c/2)\sigma_t = 0.6$ m rms. In 1-way ranging, the tone jitter at the two receptions of the ranging event may however exhibit some correlation since the differential propagation time may be smaller than the correlation time of the phase noise; e.g., an 8000 km range difference corresponds to a 0.027 sec while correlation times of 0.01-0.1 sec may be exhibited by the oscillator noise process as suggested by the phase noise spectral width observed for spacecraft oscillators.[4]

The effects of tone loop VCO noise in 2-way and 1-way ranging can be studied analogously, except recognizing the highpass (rather than lowpass) filtering effect of the loop so that VCO locking errors are of interest. A 0.1 deg rms locking error corresponds to a range error of 0.6 m rms in 2-way ranging, when the correlation time of the locking error is smaller than the propagation delay so that uncorrelated jitter exists at the transmission and reception of the ranging event. Again the differential propagation involved in 1-way ranging may cause error reduction through correlation effects, but there is no information available at this stage on VCO locking-error correlation time or phase-noise spectral width.

The time delay measurement in 2-way or 1-way ranging introduces quantization noise since time is quantized to integer units of the 100 MHz clock period. The omission of fractional cycles introduces a time measurement error of

$$\Delta t = \frac{n_{c\ell}}{f_{c\ell}} - \frac{n_{c\ell} + \Delta n_{c\ell}}{f_{c\ell}} = -\frac{\Delta n_{c\ell}}{f_{c\ell}} \tag{30}$$

where $\Delta n_{c\ell} = \Delta\theta/2\pi$ and may be assumed to be a uniformly-distributed random variable with uncorrelated contributions at the beginning and end of the counting interval. The rms timing error is then given by

$$\sigma_{\Delta t} = \frac{\sqrt{2}}{2\pi f_{c\ell}} \sigma_{\Delta\theta} = \frac{1}{\sqrt{6}\, f_{c\ell}} = 4 \text{ nanosec} \tag{31}$$

which corresponds to a 0.6 m rms range error and a 1.2 m rms range-difference error. The time jitter added by electronic processing circuity in the time counting operation will also contributed independent timing errors at the beginning and end of the counting interval. A 20 nanosec rms is characteristic for a 20 kHz ranging tone,[6] so that a net rms error of 3.0 m in range and 6.0 m in range-difference is introduced. The factor of two is again due to the fact that measurement errors cannot discriminate between 2-way and 1-way data, and a 1/2 arithmetic constant is introduced when converting the measured parameter $n_{c\ell}$ into range data in 2-way ranging as indicated in (25).

SUMMARY

The arithmetic and measurement errors in the determinations of the range, range rate and range difference have been identified and evaluated. These uncertainties are tabulated in Tables 11, 12 and 13 for the systems described. No direct comparison of the range difference errors and conventional range errors is attempted. The use of the new data type requires a new orbit determination scheme. Programs are now being developed to evaluate the usefulness of such data types in orbit determination.

A comparison of the measurement error contributions illustrate the predominance of thermal noise effects under low power budget conditions, with the other error sources becoming relevant for the high power budget case. The range data exhibited, in general, smaller error magnitudes than the range-difference data, but these magnitudes were equivalent and no definite conclusions can be made without accounting for the data processing and orbital determination program.

The improvement in user tracking gained by employing a G.S./TDRS/G.S. beacon has been explained. This link may also be employed for TDRS range and range rate tracking using coherent 2-way ranging concepts.

The range and range rate uncertainties are applied as noise and bias errors in most orbit determination programs. The system uncertainties evaluated in this report are summarized as root sum squared noise and bias errors in Tables 14, 15 and 16. It should be noted from Table 14 that the bias error from all three systems are equal, while the lowest noise error is contributed by the one way, high power budget system. This is primary due to the beacon compensation for the TDRS VCO noise. For the low power budget the errors are primarily due to thermal noise and are equivalent.

For the two way range measurement systems (Table 15) the coherent system is superior by a factor of 2 for the low power budget and slightly superior for the high power budget. Any conclusions regarding the range difference errors (Table 16) must await the completion of the orbit determination program using this data type.

TABLE 11
Range Rate Error Summary

Error Source	Effect	Ranging System			Remarks
		1-Way System (cm/sec)	2-Way Coherent System (cm/sec)	2-Way GRARR System (cm/sec)	
Velocity of light Uncertainty	Arithmetic	0.2	0.2	0.2	$\frac{\Delta c}{c} = 3 \times 10^{-7}$
User L.O. Long-term Drift	Arithmetic	0.07	No Effect	No. Effect	$\frac{\Delta f}{f} = 10^{-7}$ long term
G.S. Master Oscillator Long-term Drift	Arithmetic	7×10^{-5}	14×10^{-5}	14×10^{-5}	$\frac{\Delta f}{f} = 10^{-10}$ long term
Quantization Noise	Measurement	0.04	0.02	0.02	0.1 per sec data rate
	Measurement	0.4	0.2	0.2	1 per sec. data rate ($f_b + f_d = 5 \times 10^{-3} f_r$ assumed)
Time Jitter	Measurement	0.013	0.007	0.007	0.1 per sec. data rate
	Measurement	0.13	0.07	0.07	1 per sec. data rate
VCO Noise	Measurement	0.11	0.22	0.22	0.1 per sec. data rate
(1 degree rms locking error)	Measurement	1.1	2.2	2.2	1 per sec data rate (For correlation times shorter than Doppler measurement duration)
Thermal Noise					
Low Power Budget	Measurement	0.34	0.17	0.32	0.1 per sec data rate
	Measurement	3.4	1.7	3.2	1 per sec. data rate
High Power Budget	Measurement	0.034	0.017	0.032	0.1 per sec. data rate
	Measurement	0.34	0.17	0.32	1 per sec. data rate

TABLE 12
Range Error Summary

Error Source	Effect	Ranging System		Remarks
		Coherent User (meter)	GRARR User (meter)	
Velocity of light Uncertainty	Arithmetic	12	12	$\frac{\Delta c}{c} = 3 \times 10^{-7}$
G.S. Master Oscillator long-term drift	Arithmetic	0.004	0.004	$\frac{\Delta f}{f} = 10^{-10}$ long term
PL loop lag	Arithmetic	11.8	11.8	1 Hz loop bandwidth
	Arithmetic	0.47	0.47	5 Hz loop bandwidth
Thermal Noise				
(Low Power Budget)	Measurement	12	24	1 Hz loop bandwidth
	Measurement	27	54	5 Hz loop bandwidth
High Power Budget	Measurement	1.2	2.4	1 Hz loop bandwidth
	Measurement	2.7	5.4	5 Hz loop bandwidth
VCO Noise				
3 nanosec rms Jitter	Measurement	0.6	0.6	
Quantization Noise	Measurement	0.6	0.6	100 MHz clock
Time Jitter	Measurement	3.0	3.0	20 nanosec rms Jitter

TABLE 13
Range Difference Error Summary

Error Source	Effect	1-Way Ranging (meters)	Remarks
Velocity of light Uncertainty	Arithmetic	2.5	$\frac{\Delta c}{c} = 3 \times 10^{-7}$
G.S. Master Oscillator long term drift	Arithmetic	0.0008	$\frac{\Delta f}{f} = 10^{-10}$
PL loop lag	Arithmetic	23.6	1 Hz loop bandwidth
	Arithmetic	0.94	5 Hz loop bandwidth
Thermal Noise			
(Low Power Budget)	Measurement	34	1 Hz loop bandwidth
	Measurement	76	5 Hz loop bandwidth
(High Power Budget)	Measurement	3.4	1 Hz loop bandwidth
	Measurement	7.6	5 Hz loop bandwidth
VCO Noise	Measurement	< 0.6	3 nanosec rms jitter
Quantization Noise	Measurement	1.2	100 MHz clock
Time Jitter	Measurement	6.0	20 nanosec rms jitter

Table 14

Range Rate System Errors

System	Noise		Bias
	0.1 per sec Sampling Rate	1.0 per sec Sampling Rate	
High Power Budget			
1 way	0.12 cm/sec	1.2 cm/sec	0.2 cm/sec
2 way coherent	0.22 cm/sec	2.2 cm/sec	0.2 cm/sec
2 way GRARR	0.22 cm/sec	2.2 cm/sec	0.2 cm/sec
Low Power Budget			
1 way	0.34 cm/sec	3.6 cm/sec	0.2 cm/sec
2 way coherent	0.28 cm/sec	2.8 cm/sec	0.2 cm/sec
2 way GRARR	0.39 cm/sec	3.9 cm/sec	0.2 cm/sec

Table 15

Range System Errors

System	1 Hertz Loop Bandwidth		5 Hertz Loop Bandwidth	
	Noise	Bias	Noise	Bias
High Power Budget				
2 way coherent	3.3 meters	16.8 meters	4.1 meters	12.0 meters
2 way GRARR	3.9 meters	16.8 meters	6.2 meters	12.0 meters
Low Power Budget				
2 way coherent	12.4 meters	16.8 meters	27.2 meters	12.0 meters
2 way GRARR	24.2 meters	16.8 meters	54.1 meters	12.0 meters

Table 16

Range Difference System Errors

User Power	1 Hertz Loop Bandwidth		5 Hertz Loop Bandwidth	
	Noise	Bias	Noise	Bias
High Power Budget	7.0 meters	23.7 meters	9.8 meters	2.7 meters
Low Power Budget	34.5 meters	23.7 meters	76.2 meters	2.7 meters

REFERENCES

1. J. L. Cooley and A. Marlow, "Orbital Error Studies: Tracking from a Synchronous Spacecraft," NASA/GSFC X-551-69-7, January 1969.

2. J. L. Cooley, "Error Studies for Ground Tracking of Synchronous Satellites," NASA/GSFC X-551-72-30, January 1972.

3. C. A. Filippi, "Range and Range Rate Error Analysis for the ATS-F/NIMBUS-E TDRS Experiment," Final Report, Magnavox/ASAO, April 1971.

4. T. L. Grant and R. L. Cramer, "Effect of Oscillator Instability of Telemetry Signals," NASA/AMES TN-D-6442, July 1971.

5. D. B. Leeson, "Short Term Stable Microwave Sources," The Microwave Journal, June 1970.

6. GRARR Design Evaluation Report, General Dynamics R-67-042, December 1967.

7. GRARR Final Project Report, General Dynamics R-70-010, March 1970.

8. T. J. Grenchik, "Analysis of Signal and Noise Turnaround in the GRARR Transponder," NASA/GSFC X-551-69-323, August 1969.